Stem Cell Reports
Article

OPEN ACCESS

WNT/NOTCH Pathway Is Essential for the Maintenance and Expansion of Human MGE Progenitors

Lin Ma,[1,3,7] Yiran Wang,[1,3,7] Yi Hui,[1,3] Yanhua Du,[1,3] Zhenyu Chen,[1,3] Hexi Feng,[1,3] Shuwei Zhang,[1,3] Nan Li,[1,3] Jianren Song,[1,2] Yujiang Fang,[1,3] Xiangjie Xu,[1,3] Lei Shi,[1,3] Bowen Zhang,[1,3] Jiayi Cheng,[1,3] Shanshan Zhou,[1,3] Ling Liu,[1,2,3] and Xiaoqing Zhang[1,2,3,4,5,6,*]

[1]Brain and Spinal Cord Innovative Research Center, Tongji Hospital, Tongji University School of Medicine, Shanghai 200065, China
[2]Key Laboratory of Reconstruction and Regeneration of Spine and Spinal Cord Injury, Ministry of Education, Shanghai 200065, China
[3]Key Laboratory of Neuroregeneration of Shanghai Universities, Tongji University School of Medicine, 1239 Siping Road, Room 508, Shanghai 200092, China
[4]Tsingtao Advanced Research Institute, Tongji University, Shanghai 200092, China
[5]Shanghai Institute of Stem Cell Research and Clinical Translation, Shanghai 200120, China
[6]Translational Medical Center for Stem Cell Therapy, Shanghai East Hospital, Tongji University School of Medicine, Shanghai 200120, China
[7]Co-first author
*Correspondence: xqzhang@tongji.edu.cn
https://doi.org/10.1016/j.stemcr.2019.04.007

SUMMARY

Medial ganglionic eminence (MGE)-like cells yielded from human pluripotent stem cells (hPSCs) hold great potentials for cell therapies of related neurological disorders. However, cues that orchestrate the maintenance versus differentiation of human MGE progenitors, and ways for large-scale expansion of these cells have not been investigated. Here, we report that WNT/CTNNB1 signaling plays an essential role in maintaining MGE-like cells derived from hPSCs. Ablation of *CTNNB1* in MGE cells led to precocious cell-cycle exit and advanced neuronal differentiation. Activation of WNT signaling through genetic or chemical approach was sufficient to maintain MGE cells in an expandable manner with authentic neuronal differentiation potencies through activation of endogenous NOTCH signaling. Our findings reveal that WNT/NOTCH signaling cascade is a key player in governing the maintenance versus terminal differentiation of MGE progenitors in humans. Large-scale expansion of functional MGE progenitors for cell therapies can therefore be achieved by modifying WNT/NOTCH pathway.

INTRODUCTION

The medial ganglionic eminence (MGE), a transitory brain structure presents at mid-gestation during mammalian embryonic development, is a major region of the ventral telencephalon (Hu et al., 2017). The MGE generates over 70% of forebrain GABA (γ-aminobutyric acid)-ergic interneurons (INs), with diverse subtypes characterized by distinct biochemical constituents and synaptic connectivity, including parvalbumin and somatostatin (SST) neurons, as well as a minority of calretinin, nitric oxide synthase, and neuropeptide Y neurons (Kepecs and Fishell, 2014; Petilla Interneuron Nomenclature Group et al., 2008). MGE-derived INs migrate tangentially to populate the cortex, striatum, septum, and hippocampus, and play essential roles in modulating excitatory neuronal activity by local inhibition (Kepecs and Fishell, 2014; Marín, 2013; Wang et al., 2014). Increasing studies have revealed that dysregulation of IN development and the resulting excitatory-inhibitory imbalances are associated with severe developmental and psychiatric diseases, such as epilepsy, autism, schizophrenia, and Down syndrome (Chao et al., 2010; Marín, 2012). The MGE is also a major origin of ventral forebrain cholinergic neurons (FCNs), which are important for cognitive function (Fragkouli et al., 2009; Hoch et al., 2015; Marin et al., 2000; Wang et al., 2014). Deficiencies in FCNs are reported to be common cellular events leading to cognitive decline in Parkinson's disease and Alzheimer's disease (Bohnen and Albin, 2011; Whitehouse et al., 1982).

Grafting rodent embryonic MGE progenitors reconstitutes local INs- or FCNs-related neuronal circuits and shows beneficial effects in animal behavioral assays (Bráz et al., 2012; Daadi et al., 2009; Davis et al., 2015; Hunt et al., 2013; Martínez-Cerdeño et al., 2010; Perez and Lodge, 2013). A human origin of MGE-like progenitors have also been successfully yielded from human pluripotent stem cells (hPSCs), and sophisticated differentiation platforms for MGE progenitors have now been well-established by several groups, including ours (Chi et al., 2016; Li et al., 2009; Liu et al., 2013; Maroof et al., 2013; Nicholas et al., 2013; Xiang et al., 2017). More importantly, these *in vitro* produced human MGE progenitors also show significant therapeutic advances in a wide range of neurological disorders in animal models (Cunningham et al., 2014; Fandel et al., 2016; Liu et al., 2013; Yue et al., 2015). All these studies point to a promising approach of MGE progenitors-based replacement therapy in clinical use. However, quantity and quality derivation, enrichment, or cell fate manipulation of functional human MGE progenitors is still a foreseen bottleneck for their ultimate clinical application.

WNT and Sonic hedgehog (SHH) signaling are two opposed morphogens harboring determinant functions

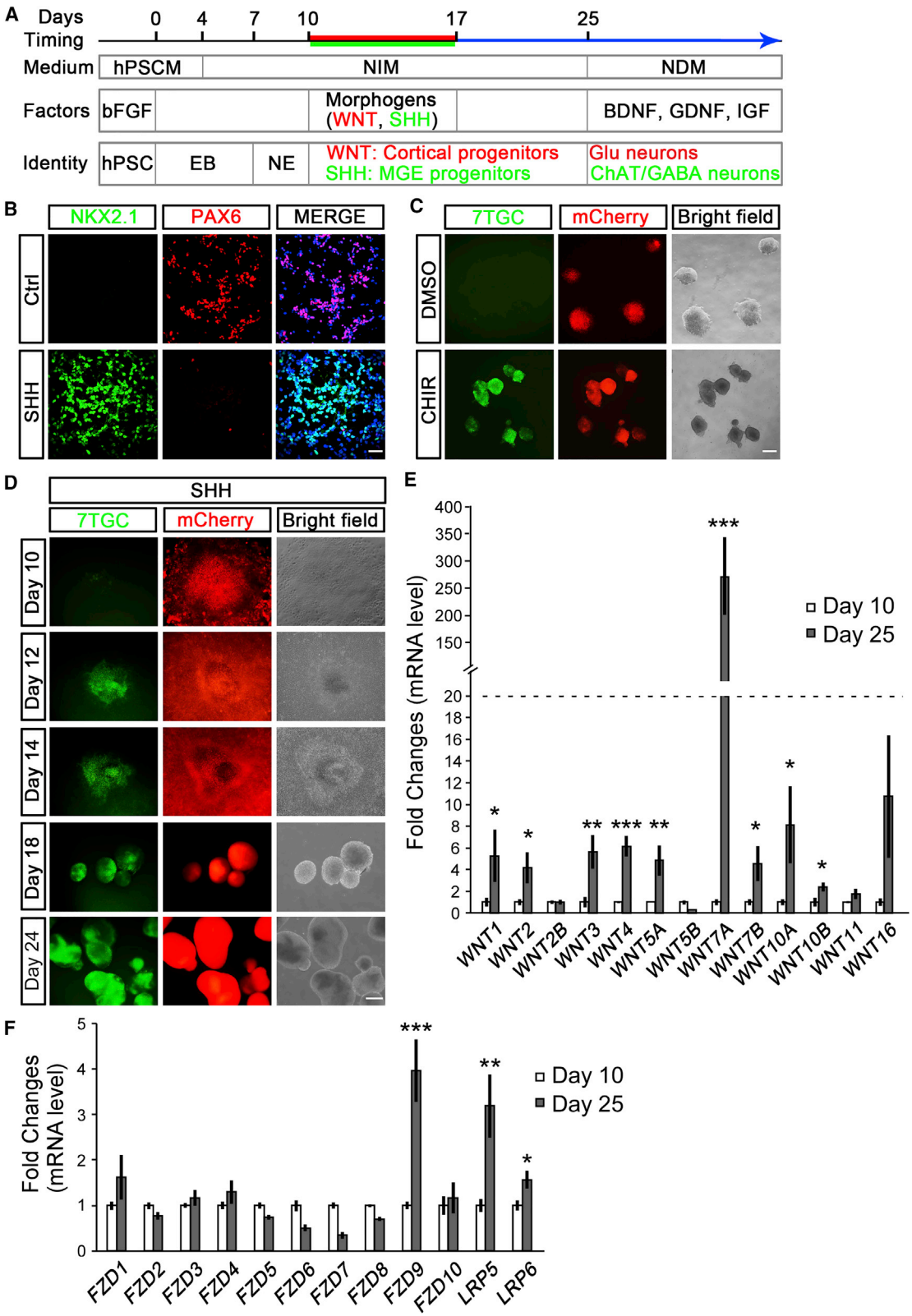

(legend on next page)

in regional specification of the dorsal and ventral telencephalon in humans, respectively (Li et al., 2009; Sur and Rubenstein, 2005). Our previous study revealed that WNT signaling inhibition facilitates SHH-triggered ventralization of human telencephalic progenitors, and therefore the ventral most human MGE progenitors could be efficiently derived from hPSCs through combined application of SHH and Dickkopf 1, a potent WNT antagonist (Li et al., 2009). Strikingly, we have also observed that an MGE fate is still adopted with even higher expression of *NKX2.1*, a hallmark gene of MGE, when both WNT and SHH signaling are concomitantly activated during the regional patterning of hPSCs (Chi et al., 2017). WNT signaling then might possess dual functions in regulating MGE regional specification, proliferation, or progenitor fate maintenance. In this study, we found that activation of WNT/CTNNB1 signaling was sufficient to maintain human MGE progenitors in an undifferentiated state, whereas ablation of WNT/CTNNB1 signaling led to precocious cell-cycle exit and advanced neurogenesis. WNT/CTNNB1 signaling transcriptionally activated NOTCH signaling pathway and therefore maintained MGE cells in a progenitor fate. Our data thus reveal a crucial role of WNT/NOTCH pathway in the maintenance of human MGE progenitors and large-scale production of functional human MGE progenitors could thus be achieved through targeting WNT/NOTCH signaling.

RESULTS

WNT/CTNNB1 Signaling Is Robustly Activated in Specified Human MGE Progenitors

Human embryonic stem cells (hESCs) were directed to cortical and MGE progenitors with our standardized protocol (Figure 1A) (Chi et al., 2016; Zhang and Zhang, 2010; Zhang et al., 2010). The yielded cortical and MGE progenitors expressed PAX6 and NKX2.1, respectively, and the mutual exclusion expression indicated the synchronization and effectiveness of the differentiation paradigm (Figure 1B). To mirror the activation of endogenous WNT/CTNNB1 signaling, we infected hESCs with the 7×Tcf-eGFP/SV40-mCherry (7TGC) reporter lentivirus, which harbors an expression cassette of GFP under the activation of seven Tcf-binding sites, and mCherry expression under the constitutively active SV40 promoter to indicate infection efficiencies (Fuerer and Nusse, 2010). In the absence of ectopic WNT activation, neuroectoderm (NEs) cells generated from 7TGC-hESCs displayed no GFP fluorescence signal (Figure 1C). Addition of CHIR99021, a WNT signaling activator, for 2 days significantly induced GFP expression, suggesting robust activation of WNT/CTNNB1 signaling (Figure 1C). It was noteworthy that, when the 7TGC-NEs were directed to an MGE fate by SHH activation from days 10 to 17 after differentiation, GFP signals started to occur at day 12 and became most prominent at day 24 (Figure 1D). At the mRNA level, several WNT ligands, especially *WNT7A*, were greatly expressed in day 25-MGE progenitors compared with their expression in day 10-NEs (Figure 1E). *FZD9*, *LRP5*, and *LRP6*, WNT receptor and co-receptors, also showed increased expression in day 25-MGE progenitors, suggesting cell-autonomous activation of WNT/CTNNB1 signaling after MGE fate specification initiated (Figure 1F).

Ablation of WNT/CTNNB1 Signaling Does Not Interfere with SHH-Initiated Specification of Human MGE Progenitors

To explore the exact role of WNT/CTNNB1 signaling in human MGE development, we knocked out *CTNNB1* in hESCs using our recently established paired-knockout (KO) strategy (Liu et al., 2016). Western blotting confirmed a complete lack of CTNNB1 protein expression in KO cells (Figure 2A). The KO-hESCs differentiated into NEs at day 10 showed uniform expression of SOX2, PAX6, OTX2, and FOXG1, similar to that of the wild-type (WT) control (Figure S1A). After continued SHH patterning from days 10 to 17, KO-NEs were also efficiently ventralized into MGE

Figure 1. Activation of WNT/CTNNB1 Signaling in Human MGE Progenitors

(A) Schematic of the procedure for generating dorsal and ventral telencephalic progenitors and neurons from hPSCs. Without ectopic morphogens, NEs were targeted to a cortical fate from days 10 to 17. For ventralization, a combination of SHH (250 ng/mL) and smoothened activator purmorphamine (0.3 μM) was added to the NE from days 10 to 17. Cortical progenitors generated glutamatergic neurons, whereas MGE progenitors produced cholinergic and GABAergic neurons.

(B) In the control (Ctrl) group, cortical progenitors expressed PAX6 but not NKX2.1 at day 17 after differentiation, whereas SHH-specified MGE progenitors only showed NKX2.1 expression. Scale bar, 50 μm.

(C) Canonical WNT signaling reporter hESCs were constructed through 7TGC lentivirus infection. Without WNT activation (DMSO), NEs derived from 7TGC-hESCs displayed no GFP fluorescence signal at day 8. Treatment with CHIR99021, a WNT activator, for 2 days significantly induced reporter GFP expression. Expression of mCherry marked lentivirus infection efficiency. Scale bar, 500 μm.

(D) MGE progenitors specified via SHH treatment in 7TGC-NEs displayed robust GFP signals as early as day 12 and persisted thereafter. Scale bar, 250 μm.

(E and F) mRNA expression of WNT ligands (E) and receptors (F) were evaluated in day 10-NEs and day 25-MGE progenitors. At least three independent experiments were performed; unpaired t test, *$p < 0.05$, **$p < 0.01$, ***$p < 0.001$.

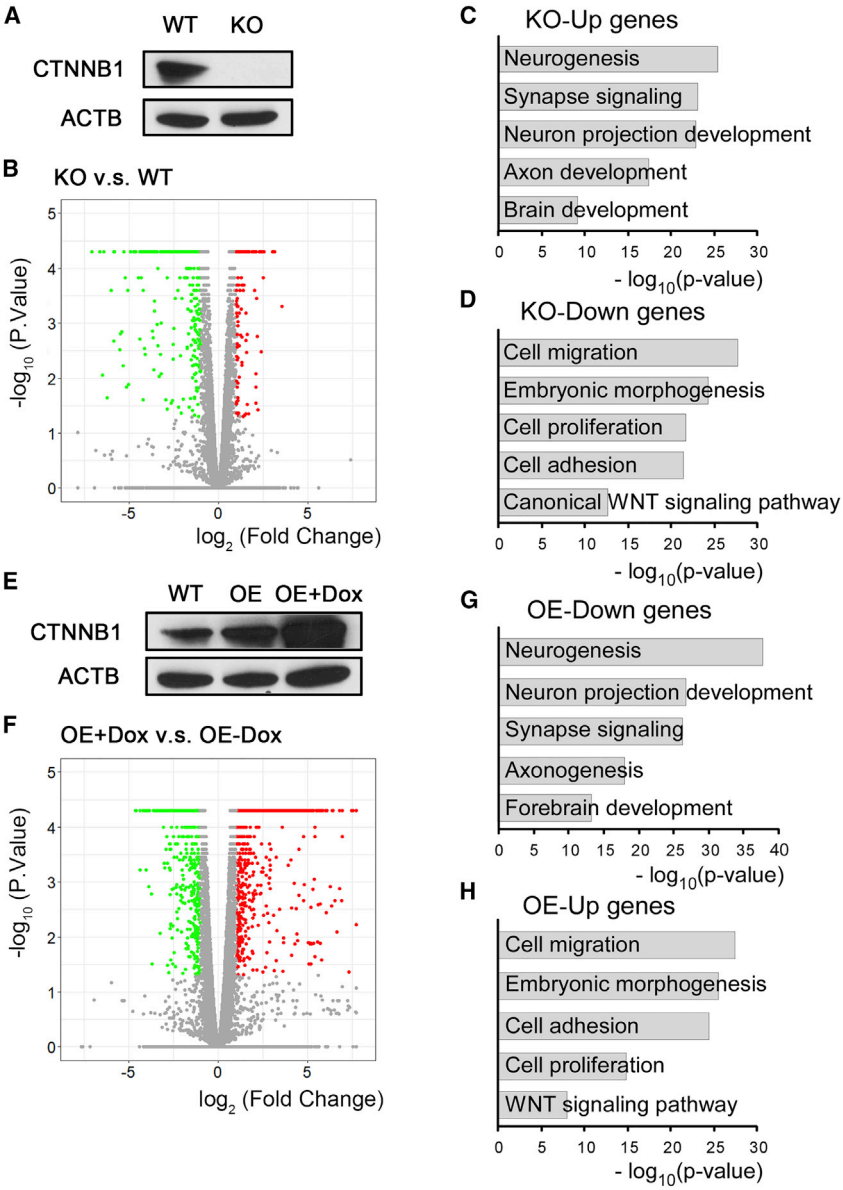

Figure 2. WNT/CTNNB1 Signaling Regulates the Progenitor Fate of Human MGE

(A) Western blotting confirmed the complete lack of CTNNB1 protein expression in knockout (KO) hESCs.

(B) WT- and KO-MGE progenitors at day 25 were subjected to RNA-seq. Volcano plot distinguished 400 upregulated and 560 downregulated differentially expressed genes (DEGs) in KO-MGE progenitors. DEGs with a fold change ≥ 1.5 and $p < 0.05$ were marked in red (upregulated) and green (downregulated).

(C and D) GO analyses of DEGs identified the functional annotations of upregulated genes (C) and downregulated genes (D) in KO-MGE progenitors.

(E) Dox-inducible *CTNNB1 S33Y* overexpression (OE) hESCs were established through lentiviral infection. Western blotting validated the effectiveness of CTNNB1 S33Y overexpression after Dox (0.1 μg/mL) treatment for 5 days.

(F) RNA-seq was performed in day 25-*CTNNB1 S33Y* OE-MGE progenitors treated with or without Dox from days 17 to 25. Volcano plot distinguished 996 upregulated and 925 downregulated DEGs in Dox-treated OE-MGE progenitors. DEGs with a fold change ≥ 1.5 and $p < 0.05$ were marked in red (upregulated) and green (downregulated).

(G and H) GO analyses identified the functional annotations of downregulated genes (G) and upregulated genes (H) in the Dox-treated group.

See also Figures S1 and S2.

progenitors with robust expression of NKX2.1 at day 25 (Figure S1B). qRT-PCR experiments confirmed robust induction of *NKX2.1* expression in both WT- and KO-MGE progenitors induced by SHH at day 25 (Figure S1C). These data suggest that abrogation of WNT/CTNNB1 signaling does not interfere with normal MGE fate initiation induced by SHH.

WNT/CTNNB1 Signaling Orchestrates Human MGE Progenitor Fate

To define the role of WNT/CTNNB1 activation in human MGE progenitors, we profiled the whole genome through RNA sequencing (RNA-seq) in KO- and WT-MGE progenitors at day 25. Visualization analysis confirmed the removal part of exon 3 of *CTNNB1* in the KO-MGE progenitors (Figure S2A). Data retrieved from 3 WT and 5 KO-MGE progenitors identified 960 differentially expressed genes (DEGs), including 400 upregulated and 560 downregulated genes (Figure 2B). Moreover, the DEGs clearly separated the KO- and WT-MGE progenitors, as per the principal-component analysis (PCA) plots (Figure S2B). Gene ontology (GO) analysis showed that the upregulated genes associated with the KO group were mainly related to neurogenesis, synapse signaling, neuron projection development, and axon development (Figure 2C), whereas the KO downregulated genes were enriched for cell migration, cell adhesion,

embryonic morphogenesis, cell proliferation, and canonical WNT signaling pathway (Figure 2D). These data suggest that ablation of *CTNNB1* leads to advanced terminal differentiation of human MGE progenitors. The hierarchical clustering heatmap of DEGs highlighted those representative genes attributing to GO term-enriched biological functions (Figure S2C). Specifically, neuroblast and neuronal marker genes *DCX* and *MAP2*, as well as synaptic marker genes *NRXN3*, *SNAP25*, *SYP*, and *SYT1*, were among the KO upregulated genes, whereas WNT receptor *FZD1*, NOTCH ligand and receptor *JAG1*, and *NOTCH2*, as well as cell adhesion- and epithelial mesenchymal transition (EMT)-related molecules *CDH7*, *CDH8*, *FAT4*, *FN1*, and *VIM* were among the KO downregulated genes (Figure S2C).

To fully delineate the impact of WNT/CTNNB1 activation on human MGE progenitors, we constructed a constitutively active *CTNNB1* (*S33Y*) inducible overexpression hESC (OE-hESC) line (Chi et al., 2017). Western blotting validated the OE efficacy after doxycycline (Dox) induction (Figure 2E). The OE-hESCs were then differentiated into MGE progenitors with the standard protocol. After the MGE fate had been initiated, Dox was applied at days 17–25. We then profiled the transcriptome of the day 25-OE-MGE progenitors treated with or without Dox. The increased expression of *CTNNB1* mRNA in Dox-treated OE cells was shown in Figure S2D. We identified 996 upregulated DEGs and 925 downregulated DEGs in the Dox-treated MGE progenitors compared with the no Dox treatment group (Figure 2F). PCA separated these two distinct populations of cells treated with or without Dox (Figure S2E). GO analysis showed enrichment in the biological functions of cell adhesion and proliferation in the upregulated DEGs, whereas enrichment in neurogenesis and neuron projection in the downregulated DEGs was clearly associated with OE-MGE progenitors treated with Dox (Figures 2G and 2H). The hierarchical clustering heatmap highlighted a similar panel, but in an opposite direction, of DEGs in the Dox group, compared with DEGs retrieved from the KO-MGE progenitors (Figure S2F). These findings propose that forced activation of WNT/CTNNB1 signaling intervenes in the programmed developmental process of human MGE progenitors, and the MGE progenitors with overactivated WNT/CTNNB1 signaling showed a retarded neuronal differentiation tendency.

WNT/CTNNB1 Signaling Regulates the Proliferation versus Neurogenesis of Human MGE Progenitors

Neural progenitors harbor both self-renewing capability to maintain themselves in a proliferative state and neuronal differentiation potency to generate postmitotic, region-specific neuronal subtypes. To confirm the involvement of WNT/CTNNB1 activation in regulating human MGE progenitor fate, we characterized the proliferation and differentiation states of human MGE progenitors upon WNT/CTNNB1 signaling repression or activation. After incubating the day-25 MGE progenitors with bromodeoxyuridine (BrdU) for 4 h, immunohistochemical experiments revealed that BrdU-incorporated cells were significantly decreased in the KO-MGE cells compared with those of the WT, suggesting that fewer cells have entered the S phase in the KO group (Figures 3A and 3B). Considering that Ki67-labeled cells remained in the cell cycle, while phospho-histone 3 (PH3)-labeled cells are in a mitotic state, both Ki67- and PH3-labeling assays showed that there was a significantly lower amount of KO-MGE cells that were proliferating or dividing (Figures 3A and 3B). Consistent with the profiling analysis, a remarkable larger population of KO-MGE progenitors were positively labeled with DCX (Figures 3C and 3D). When the day-25 MGE progenitors were plated on laminin-coated culture surface and continuously cultured for 1 month, at the mRNA level, a higher expression of *TUJ1*, *GAD67*, and *SST* was observed in KO cells (Figure 3E), suggesting that a premature cell-cycle exit occurs after ablation of WNT/CTNNB1 signaling.

To confirm that WNT/CTNNB1 signaling has a determinant role in regulating MGE progenitor maintenance versus differentiation after the MGE fate has been consolidated, but not a downstream effect of its typical role in regional patterning, we established a Dox-inducible *CTNNB1 S33Y* rescue (RE) hESC line on the background of *CTNNB1*-KO via lentiviral vector infection. After the addition of Dox, the CTNNB1 protein was abundantly expressed in RE cells (Figure 3F). Supplying Dox at days 17–25, after the MGE progenitor fate had been specified, profoundly increased cell populations remaining in cell cycle, and concomitantly attenuated cell populations expressed DCX (Figures 3G–3J).

Moreover, pulse BrdU labeling as well as immunostaining with Ki67, PH3, and DCX showed that Dox-treated OE-MGE progenitors had a higher proliferation rate as well as an attenuated differentiation state (Figures 3K–3N). These data reinforced the conclusion that activation of WNT/CTNNB1 signaling was sufficient to maintain the MGE progenitors and ensure their proliferation. Activation of WNT/CTNNB1 signaling in early NE could caudalize the cells and drive the cells to a hindbrain and spinal cord origin (Yamamoto et al., 2005). However, OE-MGE progenitors with or without Dox treatment retained their forebrain identity, because most cells expressed FOXG1 as well as NKX2.1, but not HOXB4, at day 25, indicating that activation of WNT/CTNNB1 signaling could not re-specify the MGE cells once their regional fate has been committed (Figures 3O and 3P).

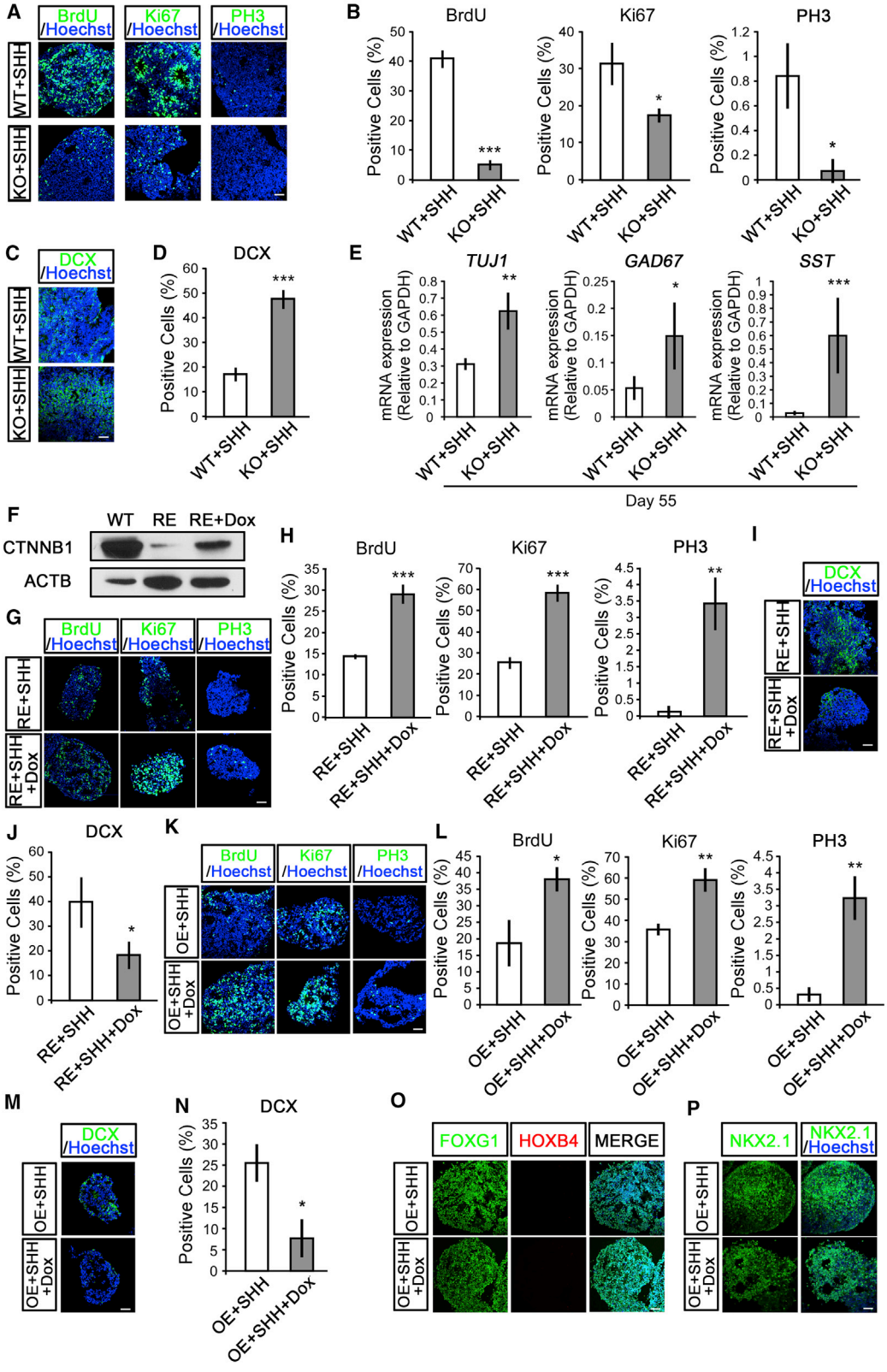

(legend on next page)

WNT/CTNNB1 Signaling Maintains MGE Progenitors through Regulating NOTCH Signaling Pathway

We then asked what are the underlying mechanisms related to WNT/CTNNB1 signaling-controlled maintenance of human MGE progenitors. There were 228 genes that were overlapped within the groups of upregulated DEGs from human KO-MGE and downregulated DEGs from OE-MGE treated with Dox (Figure 4A). There were also 207 genes that were overlapped within downregulated DEGs from the KO group and upregulated DEGs from OE cells (Figure 4B). Through protein-protein interaction (PPI) network analysis of the above overlapped genes and *CTNNB1*, we determined that *CTNNB1* was the hub gene connecting the KO downregulated genes and Dox-treated OE-MGE upregulated genes (Figure 4C). Among the 11 downregulated genes directly linked with *CTNNB1*, *NOTCH2*, and *JAG1* belonged to NOTCH signaling, *CDH7*, *CDH8*, *FAT4*, *VIM*, and *FN1* belonged to cell adhesion and EMT pathways. These data suggest that *CTNNB1* most likely maintains MGE progenitor fate through transcriptional activation of downstream genes involved in NOTCH signaling, cell-cell adhesion, and EMT pathways, which function together to constitute specific cell-cell contact niches. Gene set enrichment analysis (GSEA) showed that WNT- and NOTCH-related genes were significantly enriched in WT-MGE, but de-enriched in KO-MGE (Figures 4D and 4E). Similarly, GSEA also revealed an enrichment of WNT/NOTCH pathway-related genes in OE-MGE treated with Dox (Figures 4F and 4G). These data suggest that NOTCH signaling acts downstream of WNT/CTNNB1 signaling during human MGE development.

To further define the role of NOTCH signaling in MGE maintenance, mRNA expression of *JAG1* and *NOTCH2*, highlighted in Figure 4C, were evaluated in WT-, KO-, and OE-MGE progenitors treated with or without Dox. Indeed, *JAG1* and *NOTCH2* were remarkably attenuated in KO-MGE, and correspondingly increased in OE-MGE treated with Dox (Figure 5A). In addition, the expression of *JAG1* and *NOTCH2* was increased along with MGE specification (Figure 5B), which is in line with the activation of the WNT/CTNNB1 pathway during the differentiation of hESCs toward a MGE fate (Figures 1D–1F). To confirm the association of CTNNB1 and NOTCH signaling, chromatin immunoprecipitation (ChIP)-qPCR was performed using an inducible hemagglutinin (HA)-tagged *CTNNB1*-RE cell line. Upon addition of Dox from days 17 to 25, HA-tagged *CTNNB1*-RE-MGE progenitors were harvested at day 25. Compared with immunoglobulin G control, HA antibody pull down significantly increased fragmented DNA of *JAG1* or *NOTCH2* (Figure 5C), which indicated the recruitment of CTNNB1 to the *JAG1* and *NOTCH2* gene loci. When DAPT, a NOTCH signaling inhibitor, was added to the cultured OE-MGE progenitors in the presence of Dox from days 17 to 25, both BrdU-incorporation and Ki67-immunostaining experiments showed an effect of DAPT on reducing their proliferation (Figures 5D and 5E). Meanwhile, DAPT also significantly promoted *DCX*, *TUJ1*, and *LHX6* mRNA expression (Figure 5F), indicating a premature cell-cycle exit. These findings indicate an essential role of

Figure 3. WNT/CTNNB1 Signaling Regulates the Proliferation and Neurogenesis of Human MGE Progenitors

(A and B) Four-hour BrdU-incorporation analysis showed lower proliferation rates in KO-MGE progenitors at day 25. The KO-MGE progenitors also showed decreased Ki67 and PH3 labeling compared with that of the WT-MGE progenitors control (A). Scale bar, 50 μm. Statistical results are shown in (B). n = 236–1,027 cells in at least three independent experiments; unpaired t test, *p < 0.05, ***p < 0.001.

(C and D) Immunostaining (C) and statistical analysis (D) demonstrated that KO-MGE progenitors increased cell populations stained with DCX at day 25. Scale bar, 50 μm. n = 258–557 cells in at least three independent experiments; unpaired t test, ***p < 0.001.

(E) WT- and KO-MGE progenitors differentiated from hESCs at day 25 were plated for an additional 30 days, and mRNA expression levels of *TUJ1*, *GAD67*, and *SST* were analyzed by qRT-PCR. At least three independent experiments were performed; unpaired t test, *p < 0.05, **p < 0.01, ***p < 0.001.

(F) Construction of doxycycline (Dox)-inducible *CTNNB1 S33Y* rescue (RE) hESCs on the background of *CTNNB1*-KO was done through lentiviral vector infection. Western blotting confirmed induced expression of CTNNB1 after treatment with 0.1 μg/mL Dox for 5 days.

(G and H) Immunostaining (G) and statistical analysis (H) demonstrated that Dox treatment in RE-MGE progenitors at days 17–25 significantly increased cell populations with BrdU incorporation or Ki67 and PH3 immunolabeling. Scale bar, 50 μm. n = 85–333 cells in at least three independent experiments; unpaired t test, **p < 0.01, ***p < 0.001.

(I and J) Dox treatment in RE-MGE progenitors at days 17–25 significantly decreased cell populations immunolabeled with DCX (I). Scale bar, 50 μm. Statistical results were shown in (J). n = 130–264 cells in at least three independent experiments; unpaired t test, *p < 0.05.

(K and L) *CTNNB1 S33Y* OE-hESCs were targeted to the MGE, with 0.1 μg/mL Dox addition from day 17 to 25. At day 25, Dox-treated MGE progenitors showed increased populations of cells labeled with BrdU, Ki67, and PH3 (K). Scale bar, 50 μm. Statistical results were shown in (L). n = 98–570 cells in at least three independent experiments; unpaired t test, *p < 0.05, **p < 0.01.

(M and N) Immunostaining (M) and statistical analysis (N) demonstrated that *CTNNB1*-OE decreased cell populations immunolabeled with DCX in MGE progenitors. Scale bar, 50 μm. n = 137–271 cells in at least three independent experiments; unpaired t test, *p < 0.05.

(O) At day 25, the OE-MGE progenitors with or without Dox treatment expressed FOXG1, but not HOXB4. Scale bar, 50 μm.

(P) The OE-MGE progenitors with or without Dox treatment were immunolabeled by NKX2.1 at day 25. Scale bar, 50 μm.

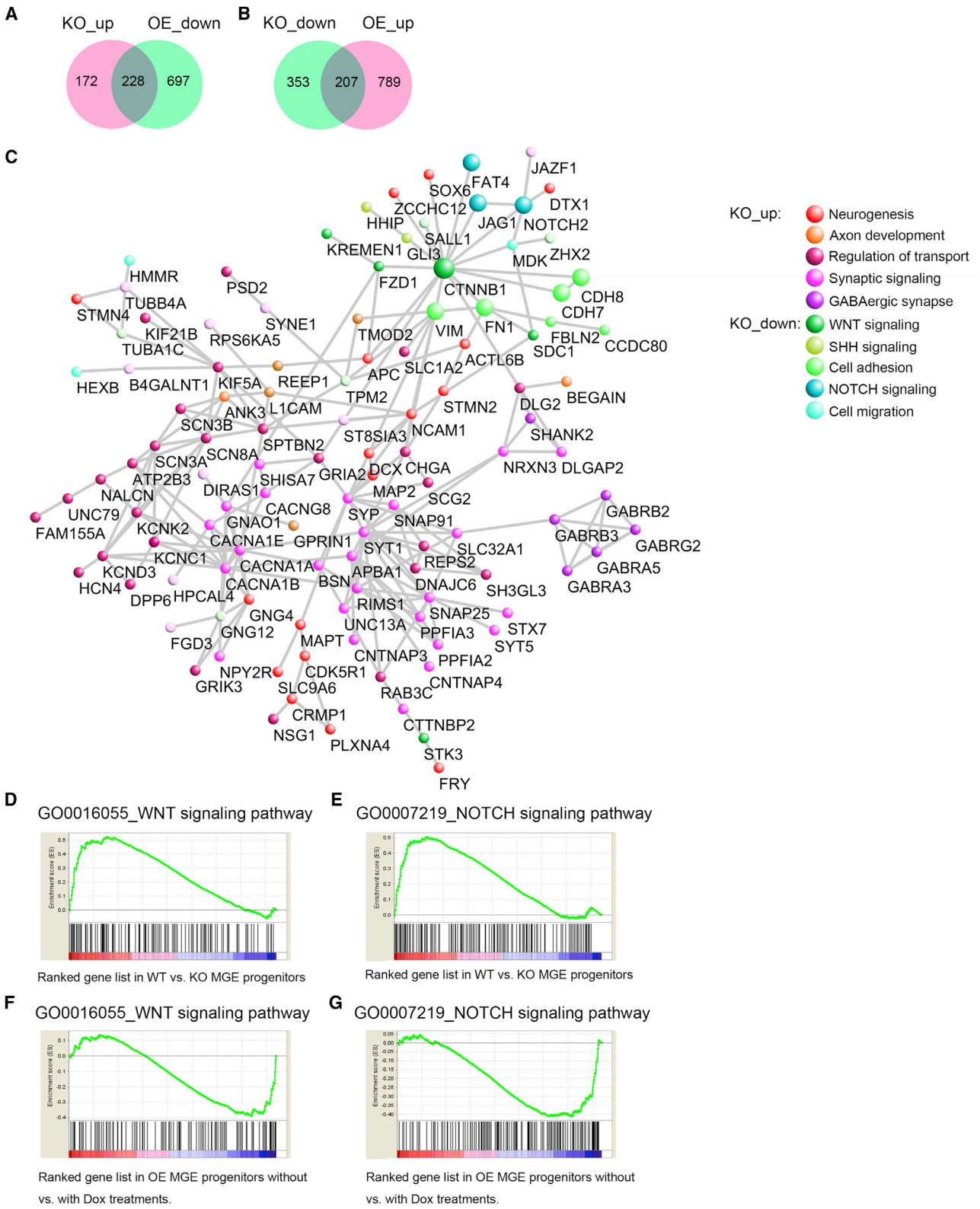

Figure 4. WNT/CTNNB1 Signaling Maintains MGE Progenitors through Regulating NOTCH Signaling Pathway

(A) In total, 228 genes were overlapped among upregulated DEGs in KO progenitors and downregulated DEGs in OE progenitors treated with Dox.

(legend continued on next page)

NOTCH signaling, which is downstream of the activated WNT/CTNNB1 pathway, in controlling the maintenance of MGE progenitors.

Long-Term Expansion of Functional Human MGE Progenitors via Chemical Activation of WNT/CTNNB1 Pathway

Large-scale production of functional MGE progenitors for replacement therapy holds the key for curing related neurological disorders. We next asked whether long-term expansion of human MGE progenitors could be achieved through manipulating the WNT/CTNNB1 signaling. CHIR99021, a WNT activator, also showed a strong effect on the maintenance and proliferation of MGE progenitors when supplied at days 17–25, as demonstrated by its strong role in increasing BrdU-incorporation rates as well as the percentage of Ki67- and PH3-labeled cells, while decreasing cell populations labeled with DCX (Figures 6A and 6B). Again, regional MGE fate was maintained in the presence of CHIR99021, because the cells retained FOXG1 and NKX2.1, but lacked HOXB4 expression (Figures 6C and 6D). Moreover, the roles of CHIR99021 on promoting the proliferation, while retarding neuronal differentiation of MGE progenitors, was also abrogated by DAPT treatment (Figures 6E–6G).

We then passaged the MGE progenitors every 7 days up to day 55 in the presence of CHIR99021 (Figure 7A). Strikingly, the sphere-shaped MGE progenitors expanded substantially upon CHIR99021 treatment, whereas cells treated with DMSO exhibited only limited expansion capacity (Figure 7B). The MGE progenitors maintained in CHIR99021 showed a larger population of cells immunolabeled with Ki67 and PH3 (Figures 7B and 7C). Similar results were observed even when the cells were cultured to day 115 with CHIR99021 (Figures 7D and 7E). Furthermore, MGE progenitors maintained with CHIR99021 consistently generated TUJ1-labeled neurons, especially SST GABAergic INs, after CHIR99021 withdrawal and being plated onto a laminin-coated surface (Figures 7F and 7G). Whole-cell patch-clamp recording of 120-day-old neuronal cultures generated from the CHIR99021-maintained MGE progenitors revealed normal resting membrane potentials and action potentials elicited by injection of current steps from +30 to +40 pA (Figures 7H and 7I). We also observed spontaneous synaptic currents in all tested cells, which were further blocked by bicuculline, a GABAa receptor antagonist (Figure 7J), thus reflecting primarily inhibitory neurotransmission inputs. These results suggest that human MGE progenitors could be efficiently expanded in the long-term through activation of WNT/CTNNB1 signaling, and these long-term expanded MGE progenitors hold desired potentials to generate functional INs.

DISCUSSION

In this study, we revealed that WNT/CTNNB1 signaling plays an important role in the maintenance of human MGE progenitors. Ablation of *CTNNB1*-mediated WNT signaling led to precocious cell-cycle exit and advanced neuronal differentiation. Ectopic activation of WNT/CTNNB1 signaling prevented neurogenesis but promoted the proliferation of MGE progenitors. This important role of canonical WNT signaling in humans could be attributed to the transcriptional activation of NOTCH signaling mediated by CTNNB1. We also proved that WNT/CTNNB1 activation could serve as a valuable strategy for large-scale expansion of MGE progenitors to yield functional INs for regenerative medicine purposes (Figure S3).

In many tissues, canonical WNT signaling is essential for the maintenance of stem cells. Typical examples include the embryonic cortex and postnatal hippocampus. Continuous activation of Wnt/Ctnnb1 signaling in mice causes massive expansion of the cerebral cortex (Chenn and Walsh, 2002; Machon et al., 2007; Wrobel et al., 2007), whereas loss of function of this pathway shows a shortened or thinner developing cerebral cortex and missing or minuscule hippocampus due to the premature cell-cycle exit of neural progenitors (Galceran et al., 2000; Lee et al., 2000; Solberg et al., 2008; Woodhead et al., 2006; Zhou et al., 2006). However, the function of the WNT/CTNNB1 signaling pathway may not be homogeneous in all types of neural progenitors. Activation of the Wnt/Ctnnb1 signaling pathway is not required for the maintenance of

(B) In total, 207 genes were overlapped among downregulated DEGs in KO cells and upregulated DEGs in OE-MGE progenitors treated with Dox.

(C) Protein-protein interaction network analysis of functional genes from the overlapping genes and *CTNNB1*. *CTNNB1* was the hub gene connecting KO downregulated genes as well as upregulated genes in OE-MGE progenitors treated with Dox, which were associated with cell-cell contact regulation, including NOTCH, cell adhesion, and epithelial mesenchymal transition pathways. Distance of dots correlated with the degree of hubness, color of dots indicated functional annotations identified by GO analyses.

(D and E) GSEA showed the enrichment of WNT (D) and NOTCH (E) signaling pathway signatures in genes enriched in WT progenitors compared with KO ones.

(F and G) GSEA showed the enrichment of WNT (F) and NOTCH (G) signaling pathway signatures in genes enriched in Dox-treated OE progenitors compared with the ones without Dox treatment.

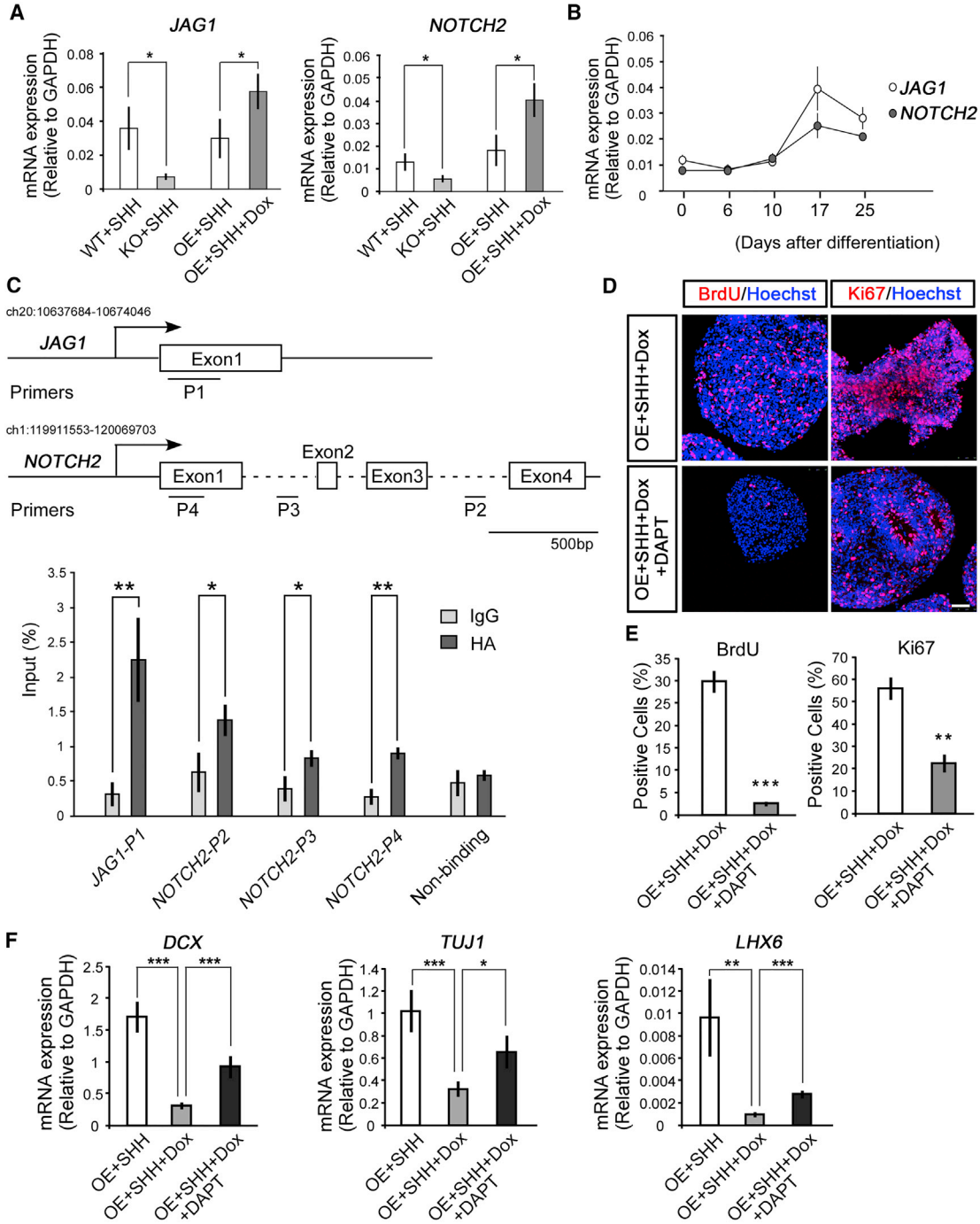

Figure 5. Inhibition of NOTCH Signaling Pathway Blocks WNT/CTNNB1-Mediated Maintenance of MGE Progenitors

(A) At the mRNA level, *JAG1* and *NOTCH2* significantly decreased in KO-MGE progenitors, while they increased in Dox-treated OE progenitors. At least three independent experiments were performed; unpaired t test, *p < 0.05.

(B) Both *JAG1* and *NOTCH2* steadily increased along with MGE specification. At least three independent experiments were performed.

(C) ChIP-qPCR showed the association of HA-tagged CTNNB1 and the indicated regions of *JAG1* and *NOTCH2*. At least three independent experiments were performed; unpaired t test, *p < 0.05, **p < 0.01.

(D and E) DAPT (50 μM), a NOTCH signaling inhibitor, was added into the medium at days 17–25, which significantly reduced the population of cells labeled with BrdU and Ki67 even when constitutive active *CTNNB1* was ectopically expressed and WNT/CTNNB1 signaling

(legend continued on next page)

hypothalamic neural progenitors, but is essential for promoting postembryonic hypothalamic neurogenesis (Duncan et al., 2016; Lee et al., 2006; Wang et al., 2009, 2012). In this study, we reveal that WNT/CTNNB1 signaling is essential for the maintenance of human MGE progenitor fate. Moreover, this role of Wnt/Ctnnb1 signaling in regulating MGE proliferation is conserved in mice (Gulacsi and Anderson, 2008). Therefore, the exact role of WNT/CTNNB1 signaling in regulating maintenance versus differentiation of neural progenitors appears to be cell-type and developmental-stage specific.

Hub gene network analysis revealed that KO downregulated genes were heavily linked with *CTNNB1*. In particular, components of NOTCH signaling, cell adhesion, and EMT pathways were significantly downregulated in the MGE progenitors with *CTNNB1* KO. GSEA further indicated NOTCH signaling was enriched in response to WNT/CTNNB1 activation. The NOTCH signaling pathway is widely manifested in the maintenance of a variety of stem cells (Androutsellis-Theotokis et al., 2006; Gaiano and Fishell, 2002; Koch et al., 2013). Moreover, WNT and NOTCH signaling pathways cooperate and integrate with each other during embryogenesis, tissue regeneration, and carcinogenesis. In most cases, the hierarchical relationship is revealed by the fact that WNT signaling transcriptionally activates the expression of NOTCH ligands (Duncan et al., 2005; Estrach et al., 2006; Hayward et al., 2008; Katoh, 2007; Katoh and Katoh, 2006; Rodilla et al., 2009), which further support our data that WNT activation resulted in upregulating of *JAG1*. Indeed, in our current research, the biological effects of *CTNNB1*-OE or CHIR99021 treatment were significantly removed by inhibition of NOTCH signaling, which abrogated the maintenance while triggered premature cell-cycle exit and neurogenesis on MGE progenitors.

MGE progenitors are valuable sources for cell transplantation to treat a wide spectrum of neurological diseases (Hu et al., 2017). While MGE progenitors can be yielded from embryonic tissues or *in vitro* differentiation of hPSCs, they will unfortunately lose their differentiation potency and gradually exit the cell cycle when expanded in culture (Holowacz et al., 2011). Here, we revealed that continuous activation of the WNT/CTNNB1 signaling pathway maintained the MGE progenitors in a proliferative state with preserved IN differentiation potency (Figure S3). Of note, the INs generated from long-term CHIR99021-maintained MGE progenitors showed functional neuronal activities and synaptic connections. Therefore, large-scale expansion of functional MGE progenitors could be achieved by modulating WNT signaling, which will greatly improve the accessibility and affordability of these cells.

EXPERIMENTAL PROCEDURES

hESC Culture and Neural Differentiation

The hESCs (WA09, WiCell) were maintained on mouse embryonic fibroblasts, and neural differentiation was performed through embryoid bodies formation (Chi et al., 2016, 2017; Fang et al., 2017; Zhang et al., 2010; Zhang and Zhang, 2010). For ventralization, a combination of SHH (250 ng/mL, R&D Systems) and the smoothened activator purmorphamine (0.3 μM, Stemgent) were added to the NE cells at days 10–17. Detailed information could also be found in Supplemental Experimental Procedures.

Generation of Mutant hESC Lines

CTNNB1 knockout and inducible OE-hESC lines were generated through CRISPR/Cas9-mediated gene editing as described previously (Chen et al., 2018; Chi et al., 2017). Inducible *CTNNB1*-RE hESCs and HA-tagged *CTNNB1*-RE hESCs were established by lentiviral infection on the background of a *CTNNB1*-KO hESC line.

RNA-Seq and Data Processing

Total RNA was isolated using TRIzol with the phenol-chloroform extraction, and RNA quality was verified using a Bioanalyzer 2100 and Qubit RNA assay kit. Total RNA (1 μg) from each sample was used to prepare a library with the NEBNext Ultra RNA Library Prep Kit for Illumina (E7530) according to the manufacturer's protocols. The libraries were then sequenced at 50 bp single read on an Illumina HiSeq 2500 platform (Chen et al., 2016, 2019; Du et al., 2017). The raw sequencing reads are available from the GEO under GEO accession number GSE112714.

Sequencing reads from each sample were mapped to the human reference genome (hg38 version) using TopHat v.2.1.1. The mapped reads were further analyzed using Cufflinks v.1.3.0 and the expression levels for each transcript were quantified as fragments per kilobase of transcript per million mapped reads.

For differential expression analysis, sequencing counts at the gene level were obtained using HTSeq v.0.9.1. R package DESeq2 was then used to identify DEGs between different conditions. To assess the significance of differential gene expression, the p value threshold was set at 0.05 and the fold change was set at 1.5.

Statistically enriched functional categories of genes were identified using DAVID 6.8 (https://david.ncifcrf.gov/). PPI networks were constructed using STRING v.10.0 (http://string-db.org/). The minimum required interaction score was set to 0.5, and others were set to default parameters. Subsequently, Cytoscape software v.3.5.1 was used for visualization of the PPI network, in which nodes represented genes and edges represented interactions between genes.

was forced activated (D). Scale bar, 50 μm. Statistical results were shown (E). n = 99–276 cells in at least three independent experiments; unpaired t test, **p < 0.01, ***p < 0.001.

(F) DAPT significantly restored OE-induced reduction of neuronal genes, including *DCX*, *TUJ1*, and *LHX6* expression in MGE progenitors. At least three independent experiments were performed; unpaired t test, *p < 0.05, **p < 0.01, ***p < 0.001.

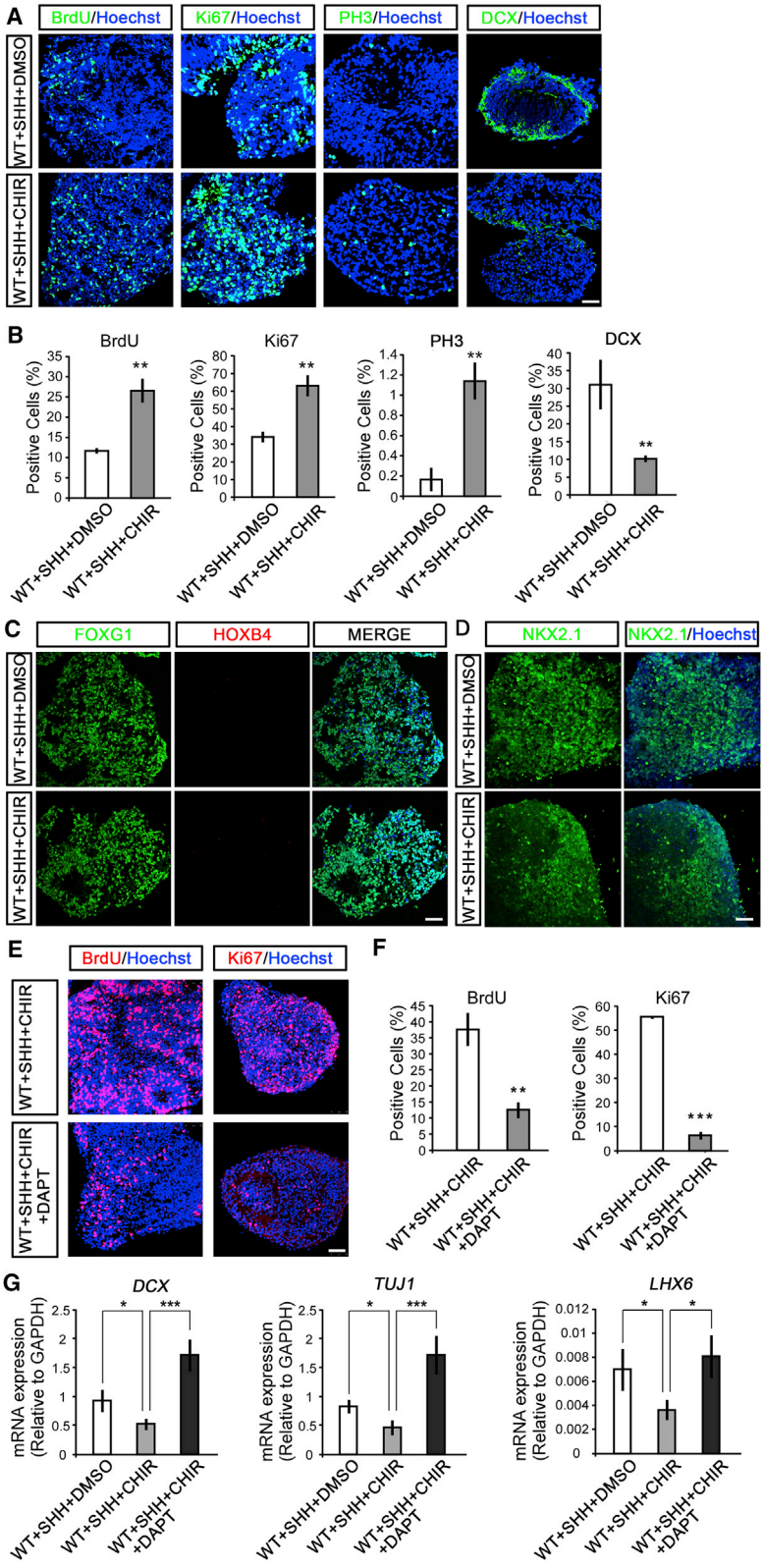

Figure 6. Chemical Activation of WNT Signaling Regulates MGE Progenitor Proliferation and Differentiation via Regulation of NOTCH Signaling

(A and B) CHIR99021 (2 μM) was added to the MGE progenitors to activate WNT/CTNNB1 signaling at days 17–25. At day 25, CHIR99021-treated MGE progenitors showed increased cell populations labeled with BrdU, Ki67, and PH3, but decreased cell populations labeled with DCX (A). Scale bar, 50 μm. Statistical results were shown in (B). n = 101–835 cells in at least three independent experiments; unpaired t test, $^{**}p < 0.01$.

(C) At day 25, the MGE progenitors treated with or without CHIR99021 showed FOXG1 staining, but not HOXB4. Scale bar, 50 μm.

(D) The MGE progenitors with or without CHIR99021 were immunolabeled by NKX2.1 at day 25. Scale bar, 50 μm.

(E and F) DAPT significantly reduced the population of cells labeled with BrdU and Ki67 upon CHIR99021-triggered WNT/CTNNB1 signaling activation (E). Scale bar, 50 μm. Statistical results were shown (F). n = 110–569 cells in at least three independent experiments; unpaired t test, $^{**}p < 0.01$, $^{***}p < 0.001$.

(G) DAPT significantly rescued CHIR99021-induced reduction of neuronal genes, including *DCX*, *TUJ1*, and *LHX6* expression in MGE progenitors. At least three independent experiments were performed; unpaired t test, $^{*}p < 0.05$, $^{***}p < 0.001$.

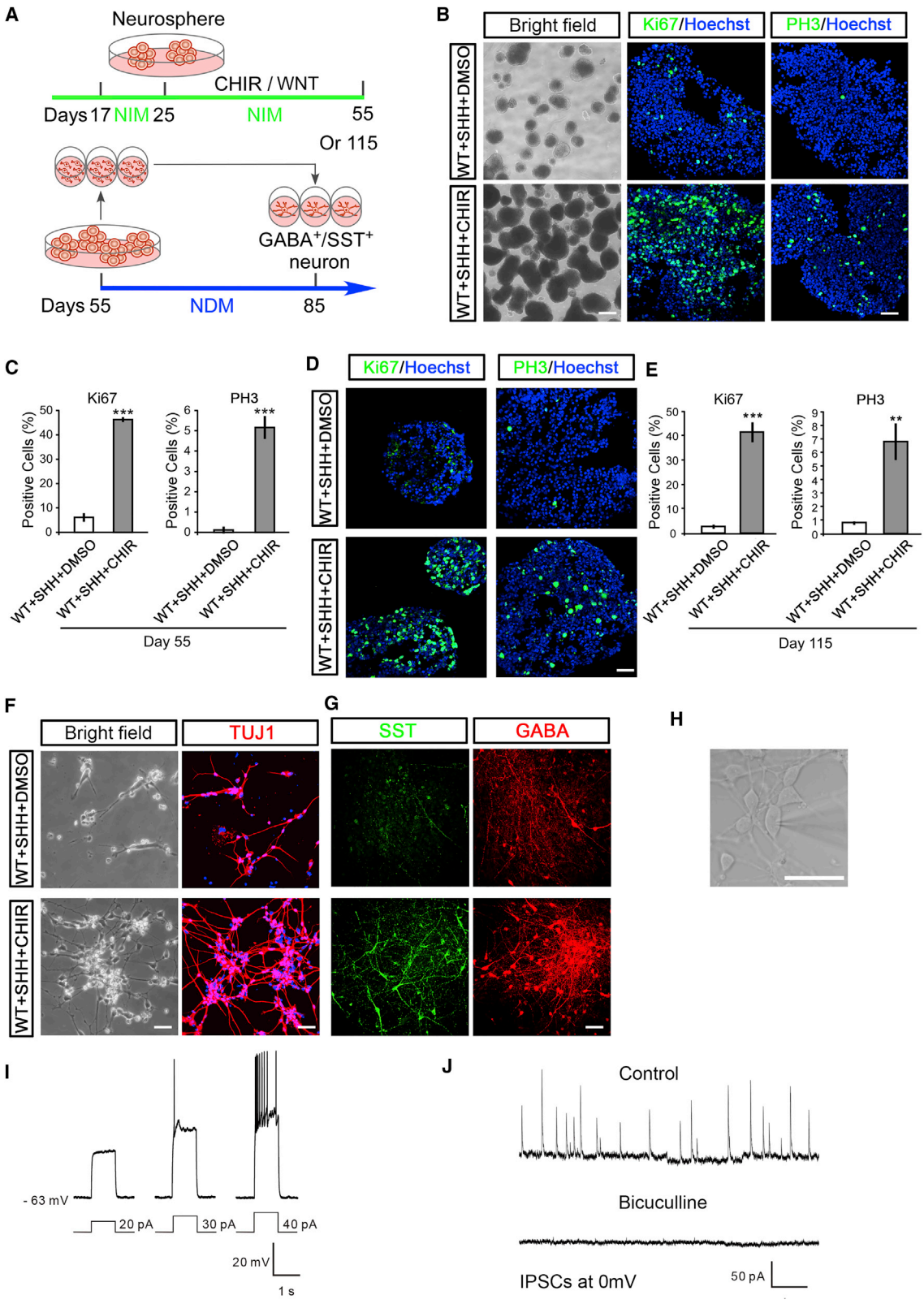

(legend on next page)

The tool GSEA (v.2.1.0) was performed to determine whether *a priori* defined set of genes shows statistically significant, concordant differences between two samples (Subramanian et al., 2005). GO gene sets were curated by The Molecular Signatures Database. Metric for ranking genes was set to Signal2Noise, and other parameters were set to default values.

Statistical Analyses

Data are presented as means ± SEM. Unpaired two-tailed Student's t test was used. Statistical significance was considered at p values below 0.05. *p < 0.05, **p < 0.01, ***p < 0.001.

SUPPLEMENTAL INFORMATION

Supplemental Information can be found online at https://doi.org/10.1016/j.stemcr.2019.04.007.

AUTHOR CONTRIBUTIONS

X.Z. conceived the study. L.M. performed most of the experiments. Y.W., Y.H., Y.D., Z.C., S. Zhang, N.L., Y.F., X.X., L.S., B.Z., J.C., S. Zhou, and L.L. helped to set up the gene targeting system and performed western blot, immunostaining, and ChIP-qPCR. J.S. performed the whole-cell recording. Y.D. and H.F. performed the bioinformatics analyses. L.M., Y.W., and X.Z. wrote the manuscript.

ACKNOWLEDGMENTS

The present study was supported by the National Key Research and Development Program of China (grant no. 2018YFA0108000), the National Natural Science Foundation of China (31400934, 31771132, 31872760, 31801204, and 31800858), the Shanghai Municipal Education Commission (C120114), the Fundamental Research Funds for the Central Universities, and the Major Program of Development Fund for Shanghai Zhangjiang National Innovation Demonstration Zone (Stem Cell Strategic Biobank and Clinical Translation Platform of Stem Cell Technology, ZJ2018-ZD-004).

Received: October 22, 2018
Revised: April 4, 2019
Accepted: April 8, 2019
Published: May 2, 2019

REFERENCES

Androutsellis-Theotokis, A., Leker, R.R., Soldner, F., Hoeppner, D.J., Ravin, R., Poser, S.W., Rueger, M.A., Bae, S.-K., Kittappa, R., and McKay, R.D.G. (2006). Notch signalling regulates stem cell numbers in vitro and in vivo. Nature *442*, 823.

Bohnen, N.I., and Albin, R.L. (2011). The cholinergic system and Parkinson disease. Behav. Brain Res. *221*, 564–573.

Bráz, J.M., Sharif-Naeini, R., Vogt, D., Kriegstein, A., Alvarez-Buylla, A., Rubenstein, J.L., and Basbaum, A.I. (2012). Forebrain GABAergic neuron precursors integrate into adult spinal cord and reduce injury-induced neuropathic pain. Neuron *74*, 663–675.

Chao, H.-T., Chen, H., Samaco, R.C., Xue, M., Chahrour, M., Yoo, J., Neul, J.L., Gong, S., Lu, H.-C., Heintz, N., et al. (2010). Dysfunction in GABA signalling mediates autism-like stereotypies and Rett syndrome phenotypes. Nature *468*, 263.

Chen, X., Zhang, K., Zhou, L., Gao, X., Wang, J., Yao, Y., He, F., Luo, Y., Yu, Y., Li, S., et al. (2016). Coupled electrophysiological recording and single cell transcriptome analyses revealed molecular mechanisms underlying neuronal maturation. Protein Cell *7*, 175–186.

Figure 7. Expansion of Functional MGE Progenitors via Chemical Activation of WNT/CTNNB1 Signaling

(A) Schematic of the procedures for long-term expansion of MGE progenitors and generation of functional INs was shown. CHIR99021 (2 μM) was maintained from day 17 to 55 or day 115, and MGE progenitors were passaged every 7 days in NIM medium. At day 55, the maintained MGE progenitors were plated on polyornithine-treated coverslips with 20 μg/mL laminin supplied with brain-derived neurotrophic factor, glial cell line-derived neurotrophic factor, and insulin-like growth factor in NDM. INs were obtained at 1 month after plating.

(B and C) At day 55, much more sphere-shaped MGE progenitors were shown in the CHIR99021-maintained culture conditions, and CHIR99021-maintained MGE progenitors showed increased populations of proliferative cells immunolabeled with Ki67 and PH3 compared with the DMSO-treated control (B). Scale bars, 500 μm (for bright field) and 50 μm (for fluorescence staining). Statistical results were shown in (C). n = 171–397 cells in at least three independent experiments; unpaired t test, ***p < 0.001.

(D and E) At day 115, CHIR99021-maintained MGE progenitors showed increased populations of proliferative cells immunolabeled with Ki67 and PH3 compared with the DMSO-treated control (D). Scale bar, 50 μm. Statistical results are shown (E). n = 89–283 cells in at least three independent experiments; unpaired t test, **p < 0.01, ***p < 0.001.

(F) One day after plating on laminin-coated culture surface, day 55-CHIR99021-maintained MGE progenitors generated neurons robustly, whereas the remaining spheres in the DMSO-treated group showed lower potentiality to generate neurons even when plated with equal cell numbers, as observed via TUJ1 immunostaining. Scale bars, 50 μm.

(G) Day 55-CHIR99021-maintained MGE progenitors generated INs at day 85 after plating, but DMSO-treated MGE progenitors showed minimized capability to generate these neurons. Scale bar, 50 μm.

(H and I) Whole-cell patch-clamp study was performed in the 120-day-old neurons differentiated from CHIR99021-treated MGE progenitors (H). Scale bar, 50 μm. Differentiated neurons showed functional action potentials, which were induced by injection of currents as low as 30 pA into neurons (I).

(J) Active spontaneous synaptic currents were captured in 120-day-old neurons differentiated from CHIR99021-treated MGE progenitors. These synaptic currents were completely blocked by bicuculline, an inhibitor of GABAa receptor.

Chen, Z., Ren, X., Xu, X., Zhang, X., Hui, Y., Liu, Z., Shi, L., Fang, Y., Ma, L., Liu, Y., et al. (2018). Genetic engineering of human embryonic stem cells for precise cell fate tracing during human lineage development. Stem Cell Reports *11*, 1257–1271.

Chen, X., Chanda, A., Ikeuchi, Y., Zhang, X., Goodman, J.V., Reddy, N.C., Majidi, S.P., Wu, D.Y., Smith, S.E., Godec, A., et al. (2019). The transcriptional regulator SnoN promotes the proliferation of cerebellar granule neuron precursors in the postnatal mouse brain. J. Neurosci. *39*, 44–62.

Chenn, A., and Walsh, C.A. (2002). Regulation of cerebral cortical size by control of cell cycle exit in neural precursors. Science *297*, 365–369.

Chi, L., Fan, B., Zhang, K., Du, Y., Liu, Z., Fang, Y., Chen, Z., Ren, X., Xu, X., Jiang, C., et al. (2016). Targeted differentiation of regional ventral neuroprogenitors and related neuronal subtypes from human pluripotent stem cells. Stem Cell Reports *7*, 941–954.

Chi, L., Fan, B., Feng, D., Chen, Z., Liu, Z., Hui, Y., Xu, X., Ma, L., Fang, Y., Zhang, Q., et al. (2017). The dorsoventral patterning of human forebrain follows an activation/transformation model. Cereb. Cortex *27*, 2941–2954.

Cunningham, M., Cho, J.-H., Leung, A., Savvidis, G., Ahn, S., Moon, M., Lee, P.K.J., Han, J.J., Azimi, N., Kim, K.-S., et al. (2014). hPSC-derived maturing GABAergic interneurons ameliorate seizures and abnormal behavior in epileptic mice. Cell Stem Cell *15*, 559–573.

Daadi, M.M., Lee, S.H., Arac, A., Grueter, B.A., Bhatnagar, R., Maag, A.-L., Schaar, B., Malenka, R.C., Palmer, T.D., and Steinberg, G.K. (2009). Functional engraftment of the medial ganglionic eminence cells in experimental stroke model. Cell Transplant. *18*, 815–826.

Davis, M.F., Figueroa Velez, D.X., Guevarra, R.P., Yang, M.C., Habeeb, M., Carathedathu, M.C., and Gandhi, S.P. (2015). Inhibitory neuron transplantation into adult visual cortex creates a new critical period that rescues impaired vision. Neuron *86*, 1055–1066.

Du, Y., Liu, Z., Cao, X., Chen, X., Chen, Z., Zhang, X., Zhang, X., and Jiang, C. (2017). Nucleosome eviction along with H3K9ac deposition enhances Sox2 binding during human neuroectodermal commitment. Cell Death Differ. *24*, 1121.

Duncan, A.W., Rattis, F.M., DiMascio, L.N., Congdon, K.L., Pazianos, G., Zhao, C., Yoon, K., Cook, J.M., Willert, K., Gaiano, N., et al. (2005). Integration of Notch and Wnt signaling in hematopoietic stem cell maintenance. Nat. Immunol. *6*, 314.

Duncan, R.N., Xie, Y., McPherson, A.D., Taibi, A.V., Bonkowsky, J.L., Douglass, A.D., and Dorsky, R.I. (2016). Hypothalamic radial glia function as self-renewing neural progenitors in the absence of Wnt/β-catenin signaling. Development *143*, 45–53.

Estrach, S., Ambler, C.A., Lo Celso, C.L., Hozumi, K., and Watt, F.M. (2006). Jagged 1 is a β-catenin target gene required for ectopic hair follicle formation in adult epidermis. Development *133*, 4427–4438.

Fandel, T.M., Trivedi, A., Nicholas, C.R., Zhang, H., Chen, J., Martinez, A.F., Noble-Haeusslein, L.J., and Kriegstein, A.R. (2016). Transplanted human stem cell-derived interneuron precursors mitigate mouse bladder dysfunction and central neuropathic pain after spinal cord injury. Cell Stem Cell *19*, 544–557.

Fang, Y., Liu, Z., Chen, Z., Xu, X., Xiao, M., Yu, Y., Zhang, Y., Zhang, X., Du, Y., Jiang, C., et al. (2017). Smad5 acts as an intracellular pH messenger and maintains bioenergetic homeostasis. Cell Res. *27*, 1083.

Fragkouli, A., van Wijk, N.V., Lopes, R., Kessaris, N., and Pachnis, V. (2009). LIM homeodomain transcription factor-dependent specification of bipotential MGE progenitors into cholinergic and GABAergic striatal interneurons. Development *136*, 3841–3851.

Fuerer, C., and Nusse, R. (2010). Lentiviral vectors to probe and manipulate the Wnt signaling pathway. PLoS One *5*, e9370.

Gaiano, N., and Fishell, G. (2002). The role of notch in promoting glial and neural stem cell fates. Annu. Rev. Neurosci. *25*, 471–490.

Galceran, J., Miyashita-Lin, E.M., Devaney, E., Rubenstein, J.L., and Grosschedl, R. (2000). Hippocampus development and generation of dentate gyrus granule cells is regulated by LEF1. Development *127*, 469–482.

Gulacsi, A.A., and Anderson, S.A. (2008). β-Catenin-mediated Wnt signaling regulates neurogenesis in the ventral telencephalon. Nat. Neurosci. *11*, 1383.

Hayward, P., Kalmar, T., and Arias, A.M. (2008). Wnt/Notch signalling and information processing during development. Development *135*, 411–424.

Hoch, R.V., Lindtner, S., Price, J.D., and Rubenstein, J.L.R. (2015). OTX2 transcription factor controls regional patterning within the medial ganglionic eminence and regional identity of the septum. Cell Rep. *12*, 482–494.

Holowacz, T., Huelsken, J., Dufort, D., and van der Kooy, D. (2011). Neural stem cells are increased after loss of β-catenin, but neural progenitors undergo cell death. Eur. J. Neurosci. *33*, 1366–1375.

Hu, J.S., Vogt, D., Sandberg, M., and Rubenstein, J.L. (2017). Cortical interneuron development: a tale of time and space. Development *144*, 3867–3878.

Hunt, R.F., Girskis, K.M., Rubenstein, J.L., Alvarez-Buylla, A., and Baraban, S.C. (2013). GABA progenitors grafted into the adult epileptic brain control seizures and abnormal behavior. Nat. Neurosci. *16*, 692.

Katoh, M. (2007). Networking of WNT, FGF, Notch, BMP, and Hedgehog signaling pathways during carcinogenesis. Stem Cell Rev. *3*, 30–38.

Katoh, M., and Katoh, M. (2006). Notch ligand, JAG1, is evolutionarily conserved target of canonical WNT signaling pathway in progenitor cells. Int. J. Mol. Med. *17*, 681–685.

Kepecs, A., and Fishell, G. (2014). Interneuron cell types are fit to function. Nature *505*, 318.

Koch, U., Lehal, R., and Radtke, F. (2013). Stem cells living with a notch. Development *140*, 689–704.

Lee, S.M., Tole, S., Grove, E., and McMahon, A.P. (2000). A local Wnt-3a signal is required for development of the mammalian hippocampus. Development *127*, 457–467.

Lee, J.E., Wu, S.-F., Goering, L.M., and Dorsky, R.I. (2006). Canonical Wnt signaling through Lef1 is required for hypothalamic neurogenesis. Development *133*, 4451–4461.

Li, X.-J., Zhang, X., Johnson, M.A., Wang, Z.-B., LaVaute, T., and Zhang, S.-C. (2009). Coordination of sonic hedgehog and Wnt

signaling determines ventral and dorsal telencephalic neuron types from human embryonic stem cells. Development *136*, 4055–4063.

Liu, Y., Weick, J.P., Liu, H., Krencik, R., Zhang, X., Ma, L., Zhou, G.-m., Ayala, M., and Zhang, S.-C. (2013). Medial ganglionic eminence-like cells derived from human embryonic stem cells correct learning and memory deficits. Nat. Biotechnol. *31*, 440.

Liu, Z., Hui, Y., Shi, L., Chen, Z., Xu, X., Chi, L., Fan, B., Fang, Y., Liu, Y., Ma, L., et al. (2016). Efficient CRISPR/Cas9-mediated versatile, predictable, and donor-free gene knockout in human pluripotent stem cells. Stem Cell Reports *7*, 496–507.

Machon, O., Backman, M., Machonova, O., Kozmik, Z., Vacik, T., Andersen, L., and Krauss, S. (2007). A dynamic gradient of Wnt signaling controls initiation of neurogenesis in the mammalian cortex and cellular specification in the hippocampus. Dev. Biol. *311*, 223–237.

Marín, O. (2012). Interneuron dysfunction in psychiatric disorders. Nat. Rev. Neurosci. *13*, 107.

Marín, O. (2013). Cellular and molecular mechanisms controlling the migration of neocortical interneurons. Eur. J. Neurosci. *38*, 2019–2029.

Maroof, A.M., Keros, S., Tyson, J.A., Ying, S.-W., Ganat, Y.M., Merkle, F.T., Liu, B., Goulburn, A., Stanley, E.G., Elefanty, A.G., et al. (2013). Directed differentiation and functional maturation of cortical interneurons from human embryonic stem cells. Cell Stem Cell *12*, 559–572.

Martínez-Cerdeño, V., Noctor, S.C., Espinosa, A., Ariza, J., Parker, P., Orasji, S., Daadi, M.M., Bankiewicz, K., Alvarez-Buylla, A., and Kriegstein, A.R. (2010). Embryonic MGE precursor cells grafted into adult rat striatum integrate and ameliorate motor symptoms in 6-OHDA-lesioned rats. Cell Stem Cell *6*, 238–250.

Marin, O., Anderson, S.A., and Rubenstein, J.L.R. (2000). Origin and molecular specification of striatal interneurons. J. Neurosci. *20*, 6063–6076.

Nicholas, C.R., Chen, J., Tang, Y., Southwell, D.G., Chalmers, N., Vogt, D., Arnold, C.M., Chen, Y.J., Stanley, E.G., Elefanty, A.G., et al. (2013). Functional maturation of hPSC-derived forebrain interneurons requires an extended timeline and mimics human neural development. Cell Stem Cell *12*, 573–586.

Perez, S.M., and Lodge, D.J. (2013). Hippocampal interneuron transplants reverse aberrant dopamine system function and behavior in a rodent model of schizophrenia. Mol. Psychiatry *18*, 1193.

Petilla Interneuron Nomenclature Group, Ascoli, G.A., Alonso-Nanclares, L., Anderson, S.A., Barrionuevo, G., Benavides-Piccione, R., Burkhalter, A., Buzsáki, G., Cauli, B., Defelipe, J., Fairén, A., et al. (2008). Petilla terminology: nomenclature of features of GABAergic interneurons of the cerebral cortex. Nat. Rev. Neurosci. *9*, 557.

Rodilla, V., Villanueva, A., Obrador-Hevia, A., Robert-Moreno, À., Fernández-Majada, V., Grilli, A., López-Bigas, N., Bellora, N., Albà, M.M., Torres, F., et al. (2009). Jagged1 is the pathological link between Wnt and Notch pathways in colorectal cancer. Proc. Natl. Acad. Sci. U S A *106*, 6315–6320.

Solberg, N., Machon, O., and Krauss, S. (2008). Effect of canonical Wnt inhibition in the neurogenic cortex, hippocampus, and premigratory dentate gyrus progenitor pool. Dev. Dyn. *237*, 1799–1811.

Subramanian, A., Tamayo, P., Mootha, V.K., Mukherjee, S., Ebert, B.L., Gillette, M.A., Paulovich, A., Pomeroy, S.L., Golub, T.R., Lander, E.S., et al. (2005). Gene set enrichment analysis: a knowledge-based approach for interpreting genome-wide expression profiles. Proc. Natl. Acad. Sci. U S A *102*, 15545–15550.

Sur, M., and Rubenstein, J.L.R. (2005). Patterning and plasticity of the cerebral cortex. Science *310*, 805–810.

Wang, X., Lee, J.E., and Dorsky, R.I. (2009). Identification of Wnt-responsive cells in the zebrafish hypothalamus. Zebrafish *6*, 49–58.

Wang, X., Kopinke, D., Lin, J., McPherson, A.D., Duncan, R.N., Otsuna, H., Moro, E., Hoshijima, K., Grunwald, D.J., Argenton, F., et al. (2012). Wnt signaling regulates postembryonic hypothalamic progenitor differentiation. Dev. Cell *23*, 624–636.

Wang, C., You, Y., Qi, D., Zhou, X., Wang, L., Wei, S., Zhang, Z., Huang, W., Liu, Z., Liu, F., et al. (2014). Human and monkey striatal interneurons are derived from the medial ganglionic eminence but not from the adult subventricular zone. J. Neurosci. *34*, 10906–10923.

Whitehouse, P., Price, D., Struble, R., Clark, A., Coyle, J., and Delon, M. (1982). Alzheimer's disease and senile dementia: loss of neurons in the basal forebrain. Science *215*, 1237–1239.

Woodhead, G.J., Mutch, C.A., Olson, E.C., and Chenn, A. (2006). Cell-autonomous β-catenin signaling regulates cortical precursor proliferation. J. Neurosci. *26*, 12620–12630.

Wrobel, C.N., Mutch, C.A., Swaminathan, S., Taketo, M.M., and Chenn, A. (2007). Persistent expression of stabilized β-catenin delays maturation of radial glial cells into intermediate progenitors. Dev. Biol. *309*, 285–297.

Xiang, Y., Tanaka, Y., Patterson, B., Kang, Y.-J., Govindaiah, G., Roselaar, N., Cakir, B., Kim, K.-Y., Lombroso, A.P., Hwang, S.-M., et al. (2017). Fusion of regionally specified hPSC-derived organoids models human brain development and interneuron migration. Cell Stem Cell *21*, 383–398.e7.

Yamamoto, A., Nagano, T., Takehara, S., Hibi, M., and Aizawa, S. (2005). Shisa promotes head formation through the inhibition of receptor protein maturation for the caudalizing factors, Wnt and FGF. Cell *120*, 223–235.

Yue, W., Li, Y., Zhang, T., Jiang, M., Qian, Y., Zhang, M., Sheng, N., Feng, S., Tang, K., Yu, X., et al. (2015). ESC-derived basal forebrain cholinergic neurons ameliorate the cognitive symptoms associated with Alzheimer's disease in mouse models. Stem Cell Reports *5*, 776–790.

Zhang, X.-Q., and Zhang, S.-C. (2010). Differentiation of neural precursors and dopaminergic neurons from human embryonic stem cells. In Human Embryonic Stem Cell Protocols, K. Turksen, ed. (Humana Press), pp. 355–366.

Zhang, X., Huang, C.T., Chen, J., Pankratz, M.T., Xi, J., Li, J., Yang, Y., LaVaute, T.M., Li, X.-J., Ayala, M., et al. (2010). Pax6 is a human neuroectoderm cell fate determinant. Cell Stem Cell *7*, 90–100.

Zhou, C.J., Borello, U., Rubenstein, J.L.R., and Pleasure, S.J. (2006). Neuronal production and precursor proliferation defects in the neocortex of mice with loss of function in the canonical Wnt signaling pathway. Neuroscience *142*, 1119–1131.

Stem Cell Reports, Volume *12*

Supplemental Information

WNT/NOTCH Pathway Is Essential for the Maintenance and Expansion of Human MGE Progenitors

Lin Ma, Yiran Wang, Yi Hui, Yanhua Du, Zhenyu Chen, Hexi Feng, Shuwei Zhang, Nan Li, Jianren Song, Yujiang Fang, Xiangjie Xu, Lei Shi, Bowen Zhang, Jiayi Cheng, Shanshan Zhou, Ling Liu, and Xiaoqing Zhang

SUPPLEMENTAL FIGURES AND LEGENDS

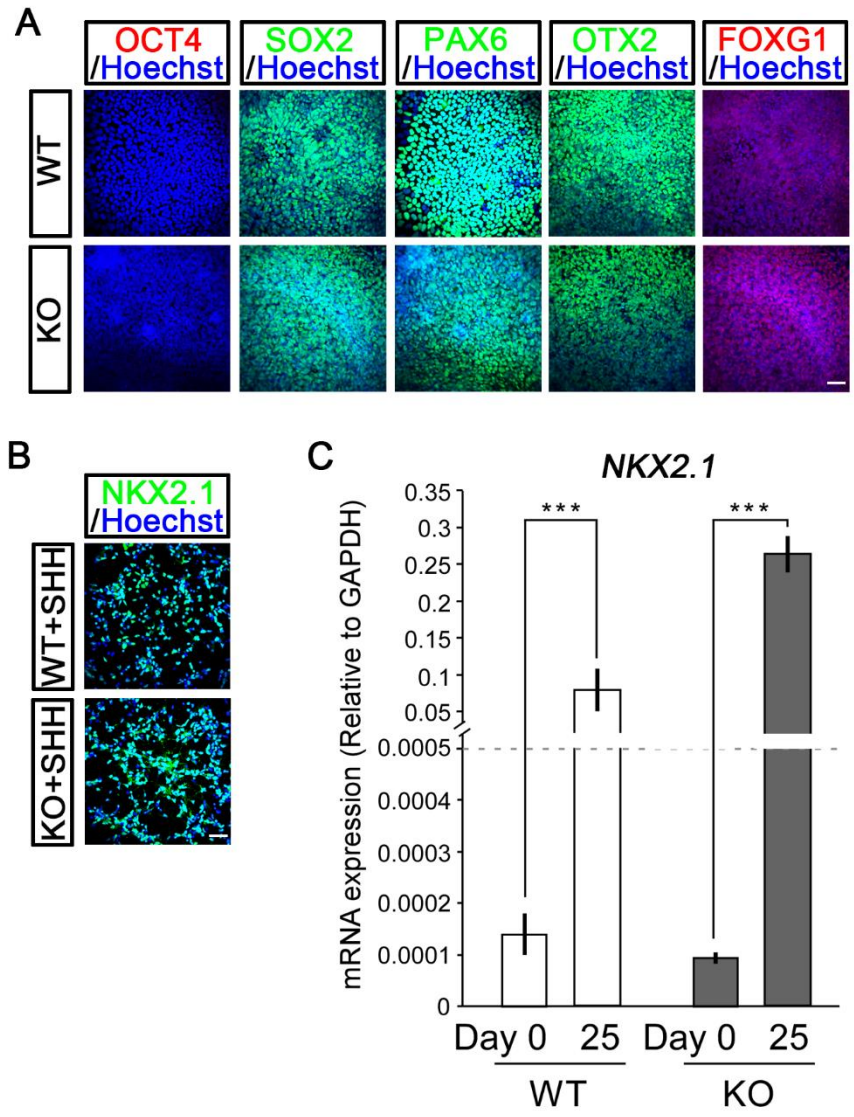

Figure S1. Ablation of WNT/CTNNB1 signaling does not interfere with SHH-initiated specification of human MGE progenitors, Related to Figure 2.

(**A**) WT- and KO-hESCs were similarly differentiated into NEs at day 10, which expressed similar profiles of NE markers, including SOX2, PAX6, OTX2, and FOXG1, but not pluripotency marker OCT4. Scale bar, 50 μm.

(**B**) Under SHH treatment, WT- and KO-hESCs efficiently differentiated into NKX2.1-positive MGE progenitors at day 25. Scale bar, 50 μm.

(**C**) At the mRNA level, both WT- and KO-MGE progenitors displayed robust expression of *NKX2.1* at day 25 as compared with the corresponding hESCs at day 0. At least three independent experiments were performed; Unpaired *t*-test, ***$P < 0.001$.

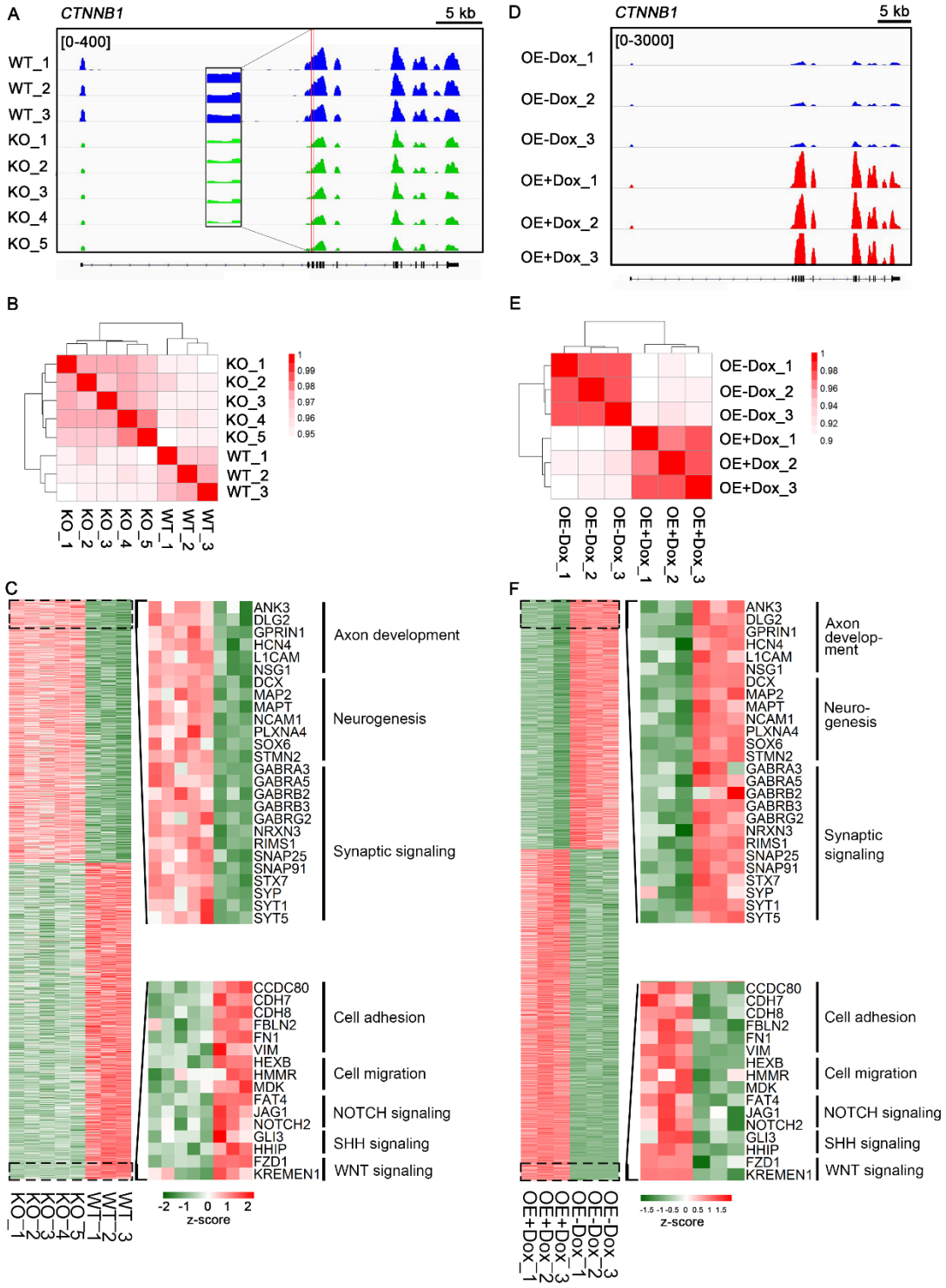

Figure S2. Expression profiles of DEGs in human WT- and KO-MGE progenitors as well as OE-MGE progenitors with or without Dox treatment, Related to Figure 2.

(**A**) Confirmation of the efficient deletion of exon 3 of *CTNNB1* in KO-MGE progenitors

by visualization analysis. Scale bar, 5 kb.

(**B**) Principal component analysis (PCA) plots clearly separated KO samples from WT controls.

(**C**) Heatmap of gene expression levels of DEGs in WT- and KO-MGE progenitors at day 25. Representative genes from GO term-enriched biological functions were listed on the right.

(**D**) Confirmation of induction of ectopic *CTNNB1* mRNA after Dox treatment through visualization analysis. Scale bar, 5 kb.

(**E**) PCA plots clearly separated OE-MGE progenitors with and without Dox treatment.

(**F**) Heatmap of DEGs showed representative genes associated with GO term-enriched biological functions.

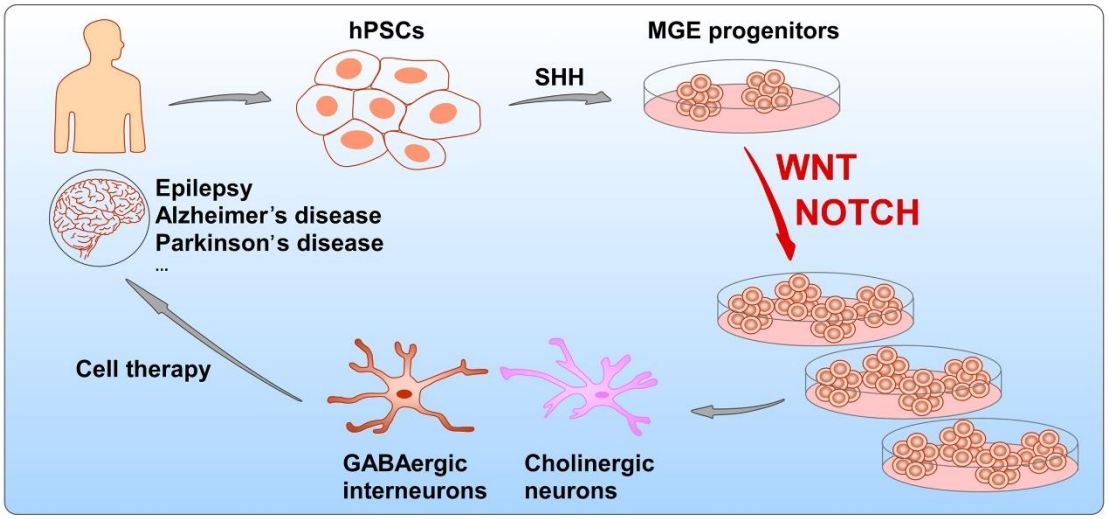

Figure S3. Schematic representation of the role and application of WNT/CTNNB1 signaling in regulating MGE progenitor maintenance, Related to Main-text.

WNT/CTNNB1 signaling played an important role in maintaining MGE progenitors in a proliferative and undifferentiated state. CTNNB1-mediated WNT signaling maintained the stemness of MGE cells by targeting NOTCH signaling pathway. Activation of WNT/CTNNB1 signaling induced expansion of human MGE progenitors, which may be able to replenish functional GABAergic and cholinergic neurons for treating neurological disorders, including epilepsy, Alzheimer's disease and Parkinson's disease.

SUPPLEMENTAL TABLE

Table S1. Primers list for qRT-PCR and ChIP-qPCR, related to **METHODS** section.

Application	Gene	Forward Primer	Reverse Primer
qRT-PCR	*GAPDH*	ATGACATCAAGAAGGTGGTG	CATACCAGGAAATGAGCTTG
qRT-PCR	*WNT1*	CGATGGTGGGGTATTGTGAAC	CCGGATTTTGGCGTATCAGAC
qRT-PCR	*WNT2*	CCGAGGTCAACTCTTCATGGT	CCTGGCACATTATCGCACAT
qRT-PCR	*WNT2B*	GGGGCACGAGTGATCTGTG	GCATGATGTCTGGGTAACGCT
qRT-PCR	*WNT3*	CTCGCTGGCTACCCAATTTG	AGGCTGTCATCTATGGTGGTG
qRT-PCR	*WNT4*	AGGAGGAGACGTGCGAGAAA	CGAGTCCATGACTTCCAGGT
qRT-PCR	*WNT5A*	ATTCTTGGTGGTCGCTAGGTA	CGCCTTCTCCGATGTACTGC
qRT-PCR	*WNT5B*	GCTTCTGACAGACGCCAACT	CACCGATGATAAACATCTCGGG
qRT-PCR	*WNT7A*	CTGTGGCTGCGACAAAGAGAA	GCCGTGGCACTTACATTCC
qRT-PCR	*WNT7B*	CACAGAAACTTTCGCAAGTGG	GTACTGGCACTCGTTGATGC
qRT-PCR	*WNT10A*	GGTCAGCACCCAATGACATTC	TGGATGGCGATCTGGATGC
qRT-PCR	*WNT10B*	CATCCAGGCACGAATGCGA	CGGTTGTGGGTATCAATGAAGA
qRT-PCR	*WNT11*	GGAGTCGGCCTTCGTGTATG	GCCCGTAGCTGAGGTTGTC
qRT-PCR	*WNT16*	TTCAGACACGAGAGATGGAACT	CCAGCCTTCACTTGCTGAG
qRT-PCR	*FZD1*	ATCTTCTTGTCCGGCTGTTACA	GTCCTCGGCGAACTTGTCATT
qRT-PCR	*FZD2*	GTGCCATCCTATCTCAGCTACA	CTGCATGTCTACCAAGTACGTG
qRT-PCR	*FZD3*	GTTCATGGGGCATATAGGTGG	GCTGCTGTCTGTTGGTCATAA
qRT-PCR	*FZD4*	CCTCGGCTACAACGTGACC	TGCACATTGGCACATAAACAGA
qRT-PCR	*FZD5*	CATGCCCAACCAGTTCAACC	CGGCGAGCATTGGATCTCC
qRT-PCR	*FZD6*	ATGGCCTACAACATGACGTTT	GTTTACGACAAGGTGGAACCA
qRT-PCR	*FZD7*	GTGCCAACGGCCTGATGTA	AGGTGAGAACGGTAAAGAGCG
qRT-PCR	*FZD8*	ATCGGCTACAACTACACCTACA	GTACATGCTGCACAGGAAGAA
qRT-PCR	*FZD9*	TGCGAGAACCCCGAGAAGT	GGGACCAGAACACCTCGAC
qRT-PCR	*FZD10*	AGCCATCCAGTTGCACGAG	GAGTCGGGCCACTTGAAGTT
qRT-PCR	*LRP5*	ACTCGCTGTGAGGAGGACAAT	GGCAGGCGCATGTGTAGAA
qRT-PCR	*LRP6*	TTTATGCAAACAGACGGGACTT	GCCTCCAACTACAATCGTAGC
qRT-PCR	*TUJ1*	GAGCGGATCAGCGTCTACTACAA	GATACTCCTCACGCACCTTGCT
qRT-PCR	*GAD67*	TGGAAGTGGTGGACATACTCC	AAGTACTTGTAGCGAGCAGCC
qRT-PCR	*SST*	CCCAGACTCCGTCAGTTTCT	TCGCTGAAGACTTGGAGGAT
qRT-PCR	*JAG1*	GTCCATGCAGAACGTGAACG	GCGGGACTGATACTCCTTGA
qRT-PCR	*NOTCH2*	CAACCGCAATGGAGGCTATG	GCGAAGGCACAATCATCAATGTT
qRT-PCR	*DCX*	TCCCGGATGAATGGGTTGC	GCGTACACAATCCCCTTGAAGTA
qRT-PCR	*LHX6*	GGGCGCGTCATAAAAAGCAC	TGAACGGGGTGTAGTGGATGT

ChIP-qPCR	*JAG1-P1*	CCTCCCGGCTTTCTTTCCTTC	CACGCGTCATTGTGTTACCTG
ChIP-qPCR	*NOTCH2-P2*	TGTTAGGACCTGAAAGGTGGTG	GATTTGCACATCAGGACTGCTAC
ChIP-qPCR	*NOTCH2-P3*	AGAAGTGCACCTGGGAATGC	CGACATCCCTGAAGGTTCCA
ChIP-qPCR	*NOTCH2-P4*	CCCTCCTCCTGCTTCAAAGG	TTCGTTGCACACCCGAGAAA
ChIP-qPCR	*Non-binding*	AGTGGTGATGAATTCCCTCAG	AATCCCCATCAGACTAACAGC

SUPPLEMENTAL METHODS

Human embryonic stem cell (hESC) culture and neural differentiation

The hESCs (WA09, WiCell) were cultured on a feeder layer of irradiated mouse embryonic fibroblasts (MEF). Cells were expanded every 5 days through dispase (Gibco, 17105) digestion. The culture medium for hPSCs (hPSCM) consisted of 392.5 ml of DMEM/F12, 100 ml of knockout serum replacer, 5 ml of MEM non-essential amino-acid solution, 2.5 ml of 200 mM L-glutamine solution, and 3.5 µl of 14.3 M β-mercaptoethanol, supplemented with 4 ng/ml FGF2.

For neural differentiation, hESCs were broken into small clumps and suspended in hPSCM for 4 days to form embryoid bodies (EBs). The EBs were then switched to neural induction medium (NIM, 489 ml of DMEM/F12, 5 ml of N2 supplement, 5 ml of MEM non-essential amino-acid solution, and 1 ml of 1 mg/ml heparin) to direct cells toward a neuroectoderm (NE) fate for 2 days. During that period, SB431542 (2 µM, Stemgent) and LDN193189 (200 nM, Stemgent), inhibitors to block TGF-β and BMP signaling, respectively, were added to the EBs from days 0 to 6. At day 6, cell aggregates were plated on laminin-coated culture surface and neural tube-like rosettes could be seen at days 14-17. For ventralization, a combination of SHH (250 ng/ml, R&D Systems) and the smoothened activator purmorphamine (0.3 µM, Stemgent) were added to the NE cells at days 10-17. The neural progenitors were maintained in suspension culture as neurospheres in NIM at day 18 through 25. At day 25, neurospheres were broken into single cells or small clusters and then plated on precoated coverslips or plates supplied with brain-derived neurotrophic factor (BDNF), glial cell line-derived neurotrophic factor (GDNF), and insulin-like growth factor (IGF)

in neural differentiation medium (NDM, 485 ml of neurobasal, 5 ml of N2 supplement, 10 ml of B27 supplement, 1 μg/ml laminin, 0.1 μM cAMP, and 200 μg/L ascorbic acid).

Generation of WNT-reporter hESC lines

The 7×Tcf-eGFP/SV40-mCherry WNT reporter in a lentiviral vector backbone was purchased from Addgene (24304). For lentivirus production, 10 μg of lentiviral WNT reporter construct, 7.5 μg of Pax2 and 5 μg of VSVG plasmids were co-transfected into HEK293FT cells (Invitrogen) cultured in a 10 cm dish using the calcium phosphate precipitation method. 16 h post transfection, fresh cell culture medium were supplied. After 2 days, the medium containing viral particles was collected and filtered through a 0.45 μm filter (Millipore). The viral particles were further concentrated by ultracentrifugation (SW28 rotor, Beckman) at 55,000 g for 3 h. The pellet was resuspended in hPSCM. For transduction, hESCs were passaged normally and pelleted by brief centrifugation. Cell pellets were then incubated with 200 μl of concentrated virus at 37°C for 30 min. The virus and cell mixture were then transferred to a MEF feeder layer overnight and fresh medium was supplied on the next day. Infected cells were selected by mCherry expression using fluorescence microscope (Olympus).

Immunohistochemistry and BrdU labeling analysis

For coverslip cultures, cells were fixed in 4% paraformaldehyde for 10 min at room temperature. For neurospheres, progenitor cells were fixed in 4% paraformaldehyde for 30 min at room temperature, and replaced with 30% sucrose for 3 h. Neurospheres were fast-frozen at -80°C until use. The neurospheres were cut on a cryostat at a thickness of 8 μm. Immunofluorescence labeling was performed by blocking the samples with 10% donkey serum in PBST (0.2% Triton X-100 in phosphate-buffered saline) for 1.5 h at room temperature, followed by incubation with primary antibodies for 36-48 h at 4°C. After washing, samples were incubated with fluorescently conjugated secondary antibodies (1:1,000, Jackson, West Grove, PA, USA) overnight at 4°C. Nuclei were counterstained with Hoechst 33258 for 10 min at room temperature.

Stained samples were washed and cover-slipped with Fluoromount-G® (SouthernBiotech, USA). Images were collected using a Leica TSC SP5 (Leica Microsystems, Bensheim, Germany) confocal laser-scanning microscope. Antibodies used included GFP (1:1,000, rabbit IgG, Invitrogen, A-6455), PAX6 (1:1,000, rabbit IgG, Covance, PRB-278P), NKX2.1 (1:400, mouse IgG, Chemicon, MAB5460), OCT4 (1:1,000, mouse IgG, Santa Cruz), SOX2 (1:1,000, goat IgG, R&D, AF2018), OTX2 (1:1,000, goat IgG, R&D, AF1979), FOXG1 (1:500, rabbit IgG, Abcam, ab23470), HOXB4 (1:50, mouse IgG, DSHB, I12), DCX (1:400, goat IgG, Santa Cruz, sc-8066), BrdU (1:200, rat IgG, Abcam, ab6326), Ki67 (1:500, rabbit IgG, Abcam, ab15580), PH3 (1:500, rabbit IgG, CST, 53348), TUJ1 (1:2,000, mouse IgG, Sigma, T8660), SST (1:500, goat IgG, Santa Cruz, sc-7819), GABA (1:2,000, rabbit IgG, Sigma, A2052).

For the BrdU pulse labeling to analyze cell proliferation, BrdU (10 μM, Sigma) was added to the cell medium, and neurospheres were collected at 2 h (*CTNNB1*-OE and CHIR99021-treated samples) or 4 h (*CTNNB1*-KO and *CTNNB1*-RE samples) after BrdU treatment.

Western blotting

Cells were lysed in protease inhibitor-containing RIPA buffer. Protein concentrations were standardized using the Pierce BCA Protein Assay Kit (Thermo Scientific). A total of 20 μg of total proteins was separated by SDS-PAGE, then transferred to nitrocellulose membranes and blotted for CTNNB1 (1:1,000; mouse IgG, BD Biosciences 610154) and ACTB (1:5,000, mouse IgG, Sigma, A5316). The secondary antibodies were purchased from Jackson ImmunoResearch.

mRNA extraction and qRT-PCR

Both mRNA extraction and qRT-PCR were performed as described previously (Chi et al., 2017; Chi et al., 2016). Total RNA was isolated using a TRIzol kit (Invitrogen) and RNA concentration was determined using a NanoDrop 2000c (Thermo Scientific). Total RNA (1 μg) from each sample was reverse transcribed into cDNA using SuperScript III (Invitrogen) and subjected to qRT-PCR (Bio-Rad, CFX Connect Real-Time System)

using the Ssofast EvaGreen kit (Bio-Rad). The housekeeping gene glyceraldehyde-3-phosphate dehydrogenase (*GAPDH*) was amplified as an internal control for gene expression analysis. The primer oligonucleotides used for qRT-PCR are listed in Table S1.

ChIP-qPCR

ChIP-qPCR was conducted according to user manual of ChampionChIP PCR Array from SABiosciences (Germantown, MD, USA) and our previous study (Du et al., 2017). Briefly, ~ 2 × 10^7 cells were crosslinked with 1% formaldehyde for 10 min at room temperature, and crosslinking was terminated by addition of 125 mM glycine. Cells were harvested for lysis to isolate nuclei. Then nuclei was suspended in 500 μl of sonication buffer (1×PBS, 1% NP-40, 0.5% sodium deoxycholate, 0.1% SDS, 1 × EDTA free protease inhibitor cocktail) and sonicated for 20 rounds of 30-s on and 30-s off using Bioruptor™ UCD-200 with high grade. It is critical that the average length of the sheared chromatin is about 250 bp, with length ranging from 50–500 bp. In order to measure the concentration and length of DNA fragment, 20 μl of fragmented DNA sample were taken out for decrosslinking for at least 2 h at 65°C along with proteinase K digestion. DNA was extracted using phenol–chloroform, then was quantitively measured as well as analyzed by 1.5% agarose electrophoresis. If the size of DNA fragment met ChIP grade requirement, 15 μg of fragmented DNA sample were diluted in 500 μl of ChIP buffer (2 mM EDTA, 150 mM NaCl, 20 mM Tris-HCl (pH 8.1), 0.1% Triton X-100, 1XEDTA free protease inhibitor cocktail), from which 10 μl of mixture were taken out as 2% input. The fragmented DNA was immunoprecipitated with 3 ~ 5 μg specified antibody (anti-IgG: abcam, ab2410, anti-HA:CST; #3724) overnight at 4°C with rotation. Then, 30 μl of ChIP-Grade Protein G Magnetic Beads (CST; #9006) were added into the mixture for another 4 h. Beads were sequentially washed three times with low salt buffer (2 mM EDTA, 20 mM Tris-HCl (pH 8.1), 0.1% SDS, 1% Triton X-100, 150 mM NaCl), once with high salt buffer (2 mM EDTA, 20 mM Tris-HCl (pH 8.1), 0.1% SDS, 1% Triton X-100, 500 mM NaCl), once with LiCl wash buffer (0.25 M LiCl,

1% NP-40, 1% sodium deoxycholate, 1 mM EDTA, 10 mM Tris-HCl (pH 8.1)), and once with TE buffer (10 mM Tris-HCl (pH 8.1), 1 mM EDTA). Then beads were suspended in elution buffer (50 mM Tris-HCl (pH 8.1), 10 mM EDTA, 0.1–0.5% SDS) at 65°C for 1 h. After that, DNA of 2% input and immunoprecipited samples were decrosslinked and extracted as mentioned above. Relative signal abundance in regions of interest in sample DNA was measured by qPCR using Power SYBR. Fragmented genomic DNA or IgG-immunoprecipitated DNA was used as control sample. Relative signal enrichment was calculated using ΔΔCt method by normalizing Ct values against control sample. The ChIP-qPCR primers were listed in the Supplementary Table S1.

Whole-cell recording

An upright infrared-differential interference contrast (IR-DIC) microscope (Olympus) equipped with epi-fluorescence illumination, a CCD camera, and two water immersion objectives (10× and 60×) was used to visualize and target recording electrodes to the cells. The coverslips with cultured cells were transferred to a recording chamber filled with oxygen (95% O_2, 5% CO_2) and maintained at a temperature of 22-25°C. The cells were continuously perfused with an extracellular solution containing: 134 mM NaCl, 2.9 mM KCl, 2.1 mM $CaCl_2$, 1.2 mM $MgCl_2$, 10 mM HEPES, and 10 mM glucose, pH 7.8 adjusted with NaOH and an osmolarity of 290 mOsm. Intracellular electrodes were pulled from borosilicate glass (1.5 mm outer diameter, 0.87 mm inner diameter, Sutter) on a flaming puller (P-1000, Sutter) and filled with intracellular solution (120 mM potassium gluconate, 5 mM KCl, 10 mM HEPES, 0.0001 mM $CaCl_2$, 5 mM EGTA, 4 mM Mg_2ATP, 0.3 mM Na_4GTP, 10 mM sodium phosphocreatine, pH 7.4 adjusted with KOH, 275 mOsm) and with yielding resistances of 5-8 MΩ. Data were collected using a MultiClamp 700B amplifier and pCLAMP10 software (Molecular Devices) and filtered at 10 KHz. For current-clamp recordings, no bias current was injected. To reveal intrinsic electrophysiological properties of the target cells, 1,000-ms current pulses (step at 2 pA) were injected into the cells to induce steady-state action potential (AP). Only neurons with stable membrane potentials at or below -48 mV fired action

potentials to supra-threshold depolarizations and showed minimal changes in series resistance (<5%) were included. For miniature inhibitory postsynaptic current (mIPSC) recordings, we voltage-clamped neurons close to the reversal potential of excitation (0 mV). Bicuculline was added to the bath to block GABAergic synaptic transmission.

SUPPLEMENTAL REFERENCES

Chi, L., Fan, B., Feng, D., Chen, Z., Liu, Z., Hui, Y., Xu, X., Ma, L., Fang, Y., Zhang, Q., *et al.* (2017). The Dorsoventral Patterning of Human Forebrain Follows an Activation/Transformation Model. Cerebral Cortex *27*, 2941-2954.

Chi, L., Fan, B., Zhang, K., Du, Y., Liu, Z., Fang, Y., Chen, Z., Ren, X., Xu, X., Jiang, C., *et al.* (2016). Targeted Differentiation of Regional Ventral Neuroprogenitors and Related Neuronal Subtypes from Human Pluripotent Stem Cells. Stem Cell Reports *7*, 941-954.

Du, Y., Liu, Z., Cao, X., Chen, X., Chen, Z., Zhang, X., Zhang, X., and Jiang, C. (2017). Nucleosome eviction along with H3K9ac deposition enhances Sox2 binding during human neuroectodermal commitment. Cell Death And Differentiation *24*, 1121.